USWNet 2009

KTH-AlbaNova, Stockholm

NOVEMBER 30 - DECEMBER 1, 2009

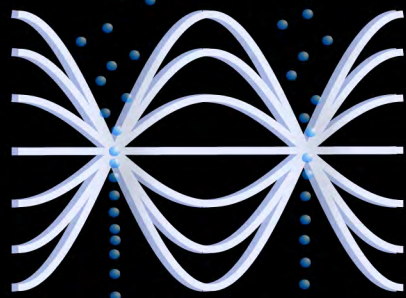

KTH VETENSKAP OCH KONST

ROYAL INSTITUTE OF TECHNOLOGY

7th Ultrasonic Standing Wave Network meeting:

"Unidirectional motion produced by vibrating fields for cell/particle and fluid control"

SCIENTIFIC PROGRAM

AND

BOOK OF ABSTRACTS

SPONSORED BY: Vetenskapsrådet

sine·phase impedance analyzers

www.uswnet.org

sine·phase

instrumentation technology

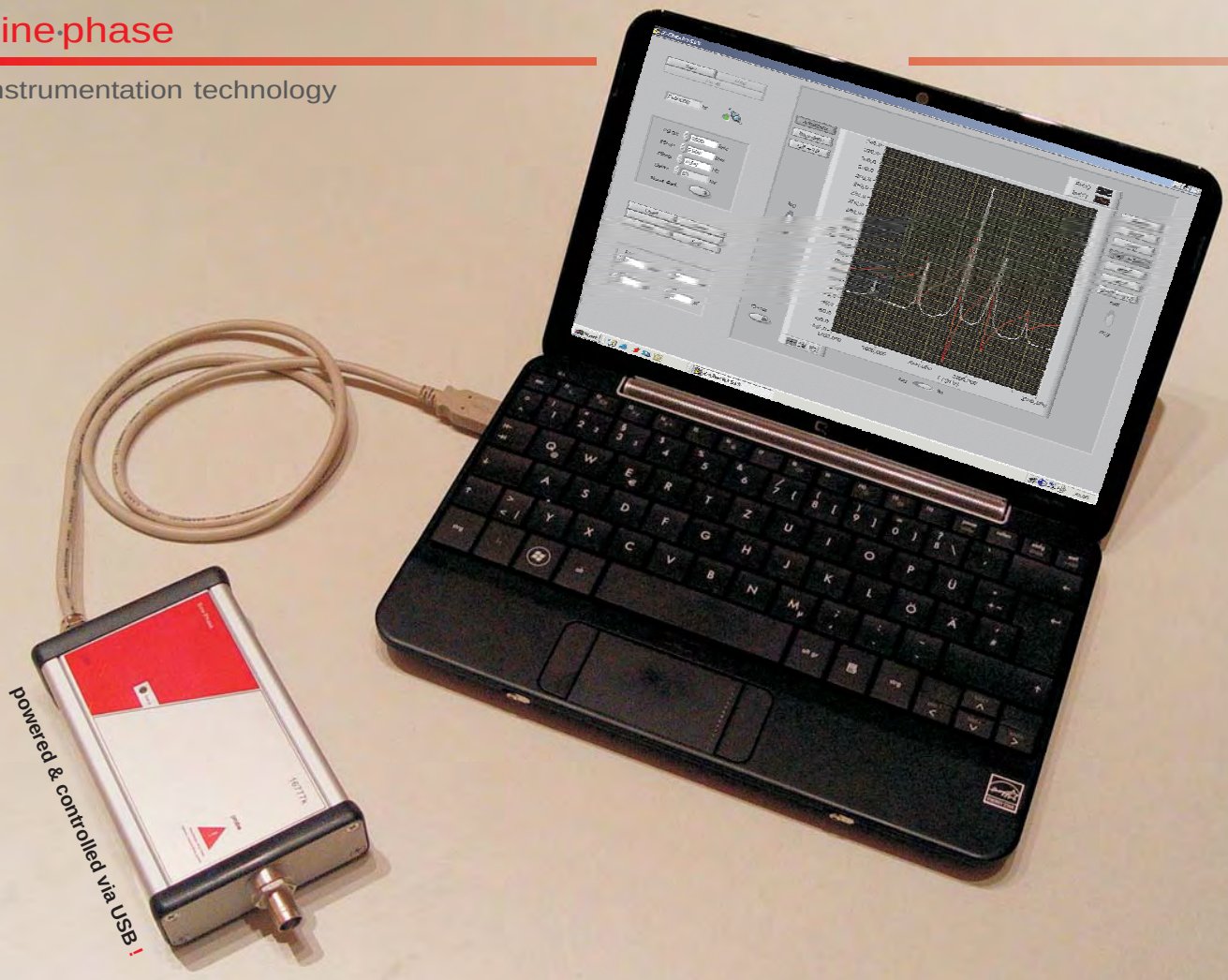

impedance Analyzer 16777k

features

+ **fully PC-controlled** - user software included
+ **netbook compliant** - also fits 1024x600 resolution
+ **power supply via USB** - no extra power supply required
+ **truely mobile** - weights less than 200 gram
+ **galvanic isolation** - for protection of your laptop, netbook, or PC
+ **data export options** - txt, bmp, jpg, png, and MS-Excel format

contact: SinePhase Instruments GmbH

Waldgasse 7
A-2371 Hinterbruehl
Austria/EUROPE
tel: (Int+43) 650 4625432
fax: (Int+43) 2236 493355

U.S. office: SinePhase USA

2112 Oak Grove Rd.
Walnut Creek, CA 94598, USA
tel: (Int+1) 925 6833673

web&mail: www.sinephase.com
info@sinephase.com

specifications

frequency range:	1 kHz to 16.777 MHz
frequ. resolution:	1 Hz
frequ. instability::	typ. < 0.001%
data range:	10 m to 100 k
	10 µS to 100 S
	0.1 pF to 10 mF
	0.1 nH to 10 H
	-90° to +90°
data resolution:	10 m 10 µS
data error (total):	typ. < 1%
power supply:	5V / 400mA (via USB)
dimensions:	126 mm x 81mm x 32mm
weight:	0.2 kg

For complete technical specifications, contact info@sinephase.com, or visit www.sinephase.com

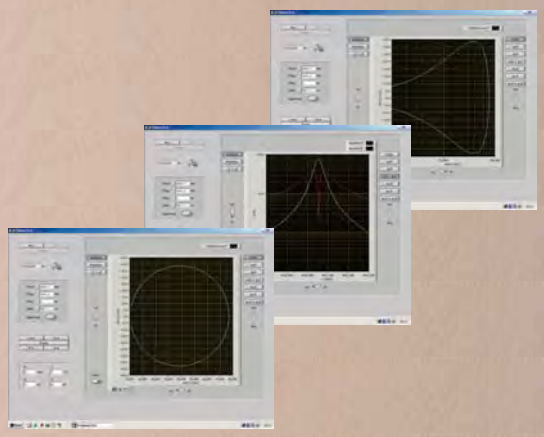

The USWNet conference organizers

Martin Wiklund	KTH Stockholm (USWNet 2009 local organizer)
Jürg Dual	ETH Zurich
Jeremy Hawkes	University of Manchester
Rosemary Boltryk	University of Southampton
Martyn Hill	University of Southampton
Stefan Radel	Vienna University of Technology

Email: meeting2009@uswnet.org

Website: www.uswnet.org

Sponsors

We gratefully acknowledge the financial contributions to the conference from:

SinePhase Instruments GmbH
Hinterbrühl, Austria
Contact person: Dr. Felix Trampler (felix.trampler@sinephase.com)
Web: www.sinephase.com and www.sonosep.com

The Swedish Research Council
Stockholm, Sweden
Web: www.vr.se

Invited speakers

Prof. Donald L. Feke, Dept. of Chemical Engineering, Case Western Reserve University, Cleveland, USA.

Prof. Feke has more than 20 years experience in USW technology and research.

Title: "*Ultrasonically driven agglomeration and coalescence phenomena in two-phase dispersions*"

Prof. Achim Wixforth, Chair for Experimental Physics, Augsburg University, Augsburg, Germany.

Prof. Wixforth is a pioneer in SAW-actuated lab-on-a-chip systems and he is a founder of the company Advalytix.

Title: "*Honey, I shrunk the lab! Acoustically driven microfluidic applications for on-chip laboratories*"

Conference venue

KTH-Albanova, Stockholm, Sweden
Address: Roslagstullsbacken 21
(see map on last page).

Oral sessions: FD5, level 4-5

Poster sessions and exhibition: B, level 4

Management meeting: FD5, level 4-5

Accomodation

Rooms have been pre-booked to a special rate at Elite Hotel Arcadia. This is a four-star, newly renovated hotel situated just in between KTH-Albanova and its nearest subway station.

Address: Körsbärsvägen 1, 114 34 Stockholm, Sweden.

Website: http://www.elite.se/eng/node/1403.

Rates: 1130 SEK (approx. 110 Euro) for one person, 1330 SEK (approx. 130 Euro) for two persons. The pre-booking and the special rates are only valid until Oct. 30, 2009. Booking is made by email (reservation.arcadia@elite.se) or phone (+46 8 566 215 00), ref. “KTH-091130”.
If you want to book another hotel or hostel, please check: http://beta.stockholmtown.com/en/.

Registration and payment

Payment: On-site payment can be done by credit card at the registration desk. The on-site conference fee is €200 and includes lunch, coffee/pastry and the conference dinner.

Registration: When you have made the payment, please provide the following information to the registration desk:

Name:	
Email address:	
Company/university:	
Address:	
Country:	

Wireless network

Wireless network is available for all participants. Individual user names and passwords are distributed at the registration desk. Network name: “AlbaNova”, choose “Users at partner Universities”; “Kungliga Tekniska Högskolan”, log in with you personal guest account valid from Nov. 30 to Dec. 1, 2009.

Conference dinner sponsored by SinePhase Instruments

The conference dinner is held on M/S Enköping. According to Lloyd's Register of Shipping, it is the oldest passenger ship still in use (built in 1868). The boat departs from Nybrokajen in the heart of Stockholm City and will take you on a cruise through the inner archipelago of Stockholm. A traditional Scandinavian Christmas buffet will be served, while you enjoy a sightseeing tour around the Royal Palace and the City Hall (where the Nobel Prize Banquet is taking place just the week after the USWNet meeting).

Enjoy a conference dinner on a boat which is as old as Kundt's tube.

Useful links

Elite Hotel Arcadia:	http://www.elite.se/eng/node/1403
Stockholm Public Transport:	http://www.sl.se/
Airport train:	https://www.arlandaexpress.com
Airport bus:	http://www.flygbussarna.se
KTH Albanova:	http://www.albanova.se/
KTH Applied Physics:	http://www.aphys.kth.se/
Stockholm visitor's guide:	http://beta.stockholmtown.com/en/

Contact address, local organizer

Martin Wiklund
KTH-Albanova
Dept. of Applied Physics
Phone: +46 8 5537 8134
Fax: +46 8 5537 8466
Email: martin@biox.kth.se

USWNet 2009 scientific program

Program overview

Nov. 30	13:00 – 13:10	Opening remarks	
	13:10 – 14:00	Invited speaker 1	Prof. D. L. Feke
	14:00 – 15:00	Oral session 1	Device design and modeling I
	15:00 – 15:45	Poster session 1	Biomedical applications I
	15:45 – 17:05	Oral session 2	Biomedical applications II
	17:20 – 18:00	Oral session 3	Bubbles
	18:00 – …	Sponsor event	Presentation and dinner
Dec. 1	08:30 – 09:20	Invited speaker 2	Prof. A. Wixforth
	09:20 – 10:00	Oral session 4	Device design and modeling II
	10:00 – 10:45	Poster session 2	Device design and modeling III
	10:45 – 12:05	Oral session 5	Acoustophoresis
	12:15 – 13:15	Oral session 6	Surface and plate waves
	13:15 – 13:30	End remarks	

Pre-program, day 1 (November 30, 2009)

WHEN	WHAT	WHERE
10:00 – 13:00	**Registration** The registration desk is located in the rotunda of the Albanova building, south entrance, level 5.	**Main entrance, level 5 (Rotunda)**
11:00 – 12:00	**Management meeting** (Chair: Jeremy Hawkes) The management meeting is open for all participants. Agenda: USWNet organization, USWNet meeting 2010, USWNet website.	**FD5**
12:00 – 13:00	**Welcome reception** A lunch buffet is served for all participants.	**A23, level 2**

Scientific program, day 1 (November 30, 2009)

13:00 – 13:10	**Opening remarks** Hans Hertz, head of KTH Applied Physics Martin Wiklund, USWNet 2009 local organizer	**FD5**	
13:10 – 14:00	**Invited talk 1** (Chair: Martin Wiklund) *"Ultrasonically driven agglomeration and coalescence phenomena in two-phase dispersions"* Donald L. Feke, Case Western Reserve University, Cleveland	**FD5**	page 9
	Oral session 1 – Device design and modeling I (Chair: Jürg Dual)	**FD5**	
14:00 – 14:20	*"Measurement of acoustic resonance line shapes by microbead acoustophoresis in straight microchannels"* Rune Barnkob, DTU Copenhagen		page 10
14:20 – 14:40	*"A thin-reflector mode for ultrasonic particle manipulation in layered resonators"* Peter Glynne-Jones, University of Southampton		page 12
14:40 – 15:00	*"Calculations for the time-averaged acoustic forces and torques experienced by a rigid cylinder in a slightly viscous fluid"* Jingtao Wang, ETH Zurich		page 14

WHEN	WHAT	WHERE	
15:00 – 15:45	**Poster session 1 - Biomedical applications I** **Exhibition: SinePhase instruments GmbH** (including coffee and pastry)	**B, level 4**	
	"Some biological applications of Ultrasound Standing Wave Systems" Despina Bazou, Trinity College Dublin	P1-1	page 15
	"Bio-suspensions in the ultrasonic h-shape filter" Cosima Koch, Vienna University of Technology	P1-2	page 17
	"Prolonged ultrasonic trapping and characterization of living cells in a microfluidic chip" Ida Iranmanesh, KTH Stockholm	P1-3	page 18
	"Ultrasonic manipulation in microfluidic systems: Selective cell handling and characterization" Jessica Svennebring, KTH Stockholm	P1-4	page 20
	Oral session 2 – Biomedical applications II (Chair: Thomas Laurell)	**FD5**	
15:45 – 16:05	*"Highly parallelized cell aggregation by ultrasound for studies of immune cell interaction"* Bruno Vanherberghen, KTH Stockholm		page 22
16:05 – 16:25	*"USW manipulating the location of suspended yeast cells in close proximity to an in-line infrared spectroscopy probe"* Stefan Radel, Vienna University of Technology		page 24
16:25 – 16:45	*"Cell trapping in single-use capillaries with MALDI-MS readout"* Björn Hammarström, Lund University		page 26
16:45 – 17:05	*"Cylindrical standing wave resonator for liquid food quality control"* Aba Priev, Hebrew University, Jerusalem		page 28
17:05 – 17:20	**Break**		
	Oral session 3 - Bubbles (Chair: Jeremy Hawkes)	**FD5**	
17:20 – 17:40	*"Bubble motion and self organisation in a microfluidic channel in the presence of ultrasonic standing waves"* David Rabaud, University of Joseph Fourier, Grenoble		page 29
17:40 – 18:00	*"Cavitation bubble structures in a standing ultrasonic wave and their cleaning potential"* Andrea Otto, Georg-August University, Göttingen		page 31
18:00 – 18:15	**Sponsor presentation** (Chair: Martin Wiklund) **"***Blind power, true power, and efficacy of an ultrasonic separator based on impedance spectrum measured"* Felix Trampler, SinePhase Instruments GmbH	**FD5**	
18:15 – 19:15	**Break** Transport by foot from Albanova to Elite Hotel Arcadia.		

Conference dinner on M/S Enköping (sponsored by SinePhase Instruments)

Enjoy a traditional Swedish Christmas Buffet on the world's oldest ship: M/S Enköping!

19:15 (sharp)	Bus departure from Elite Hotel Arcadia
19:45 (sharp)	M/S Enköping departs from Nybrokajen, kajplats 6
22:45 (approx.)	M/S Enköping returns to Nybrokajen, bus transport back to the hotel
23:00 (approx.)	Bus returns to Elite Hotel Arcadia

Scientific program, day 2 (December 1, 2009)

WHEN	WHAT	WHERE	
08:30 – 09:20	**Invited talk 2** (Chair: Rosie Boltryk)	**FD5**	
	"Honey, I shrunk the lab! Acoustically driven micro-fluidic applications for on-chip laboratories" Achim Wixforth, University of Augsburg		page 33
	Oral session 4 – Device design and modeling II (Chair: Rosie Boltryk)	**FD5**	
09:20 – 09:40	*"Rotation of non spherical particles with amplitude modulation"* Thomas Schwarz, ETH Zurich		page 34
09:40 – 10:00	*"Control of the unidirectional particle motion in a channel within a vibrating multilayer plastic micro-device"* Icíar González, CSIC Madrid		page 36
10:00 – 10:45	**Poster session 2 – Device design and modeling III** **Exhibition: SinePhase instruments GmbH** (including coffee and pastry)	**B, level 4**	
	"Reducing particle size dispersion in free flow acousto-phoresis using 2D acoustic prefocusing" Carl Grenvall, Lund University	P2-1	page 38
	"Modelling of a standing surface acoustic wave device for flow cytometry in an oceanographic sensor" Michael Gedge, University of Southampton	P2-2	page 40
	"Flow-free transport of particles in a macro scale chamber" Dirk Möller, ETH Zurich	P2-3	page 42
	"Characterization of acoustic streaming in an ultrasonic cage" Mathias Ohlin, KTH Stockholm	P2-4	page 43
	"An ultrasonic particle trap using 3-D structures" Rosie Boltryk, University of Southampton	P2-5	page 45
	Oral session 5 – Acoustophoresis (Chair: Stefan Radel)	**FD5**	
10:45 – 11:05	*"Acoustic evaluation of ion-exchange dynamics using a single resin bead"* Tetsuo Okada, Tokyo Institute of Technology		page 47
11:05 – 11:25	*"Characterising a particle trap for the monitoring of ion-exchange processes"* Rosie Boltryk, University of Southampton		page 49
11:25 – 11:45	*"Separation of particles by using an acoustic program-ming field in SPLITT channels"* Mauricio Hoyos, ESPCI Paris		page 51
11:45 – 12:05	*"Acoustic whole blood plamsapheresis chip for PSA microarray diagnostics"* Andreas Lenshof, Lund University		page 52
12:05 – 12:15	**Break**		

WHEN	WHAT	WHERE	
	Oral session 6 – Surface and plate waves (Chair: Martyn Hill)	**FD5**	
12:15 – 12:35	*"Three devices for SAW-induced particle manipulation in continuous flow systems"* Linda Johansson, Uppsala University		page 54
12:35 – 12:55	*"Drop mixing and displacement by surface acoustic waves"* Philippe Brunet, IEMN Lille		page 56
12:55 – 13:15	*"Movement of liquids and solid particles on resonating plates"* Jeremy Hawkes, University of Manchester		page 58
	End remarks (Chair: Jeremy Hawkes)	**FD5**	
13:15 – 13:20	Jeremy Hawkes, USW summer course 2010 Coordinator		
13:20 – 13:25	Rosie Boltryk, USWNet website manager		
13:25 – 13:30	Thomas Laurell, USWNet 2010 local organizer		

Building overview: Albanova University Center

(map of Stockholm: page 59)

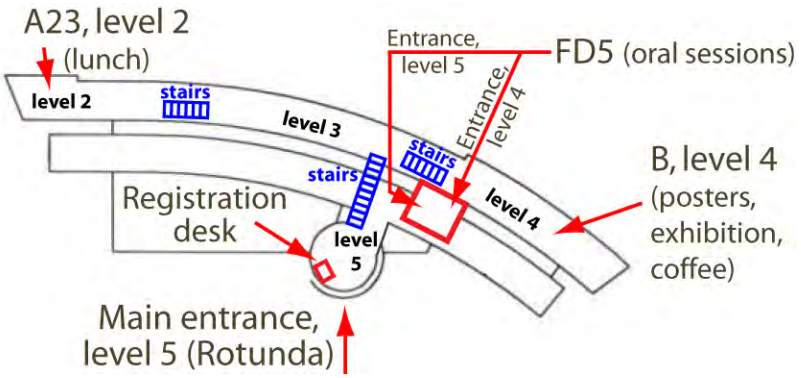

Registration (day 1):	**Main entrance level 5 (Rotunda)**
Lunch (day 1):	**A23, level 2**
Management meeting (day 1):	**FD5, level 4-5**
Conference room, oral sessions (day 1 and 2):	**FD5, level 4-5**
Poster sessions (day 1 and 2):	**B, level 4**
Exhibition, SinePhase Instruments (day 1 and 2):	**B, level 4**
Coffee and pastry during poster session, exhibition and breaks (day 1 and 2):	**B, level 4**

Ultrasonically Driven Agglomeration and Coalescence Phenomena in Two-Phase Dispersions

Donald L. Feke

Department of Chemical Engineering
Case Western Reserve University
Cleveland, Ohio 44106-7217
U.S.A.
donald.feke@case.edu

Ultrasonic standing wave fields can be used to provide the basis for approaches to control the state of agglomeration in particle suspensions or to control coalescence phenomena in liquid-liquid and gas-liquid emulsions. In this presentation, recent advances in understanding of the fundamental phenomena underlying agglomeration and coalescence processes driven by ultrasonic standing wave fields will be described. Models applying at two distinct length scales have been developed to predict tendencies for, and rates of agglomeration and coalescence. The results of various experiments that corroborate the model predictions will also be presented.

One category of model applies at the microscopic level (i.e., at the length scale of individual particles) and is used to predict the relative velocity of a pair of particles (solid, liquid, or gas) toward an agglomeration or coalescence event, or between an individual particle and substrates positioned within the ultrasonic field. Forces associated with gravity (weight and buoyancy) and the primary acoustic force determine the relative approach until the particle is a few radii from collision with its target. Subsequently, additional interparticle effects (such as van der Waals forces and secondary acoustic forces) contribute to the relative trajectory. Experiments designed to enable observation and video tracking measurements of the relative approach of two particles have been performed under a variety of operating conditions to validate the model predictions. Figure 1 shows an example of the coalescence of two air bubbles suspended in water under the application of a one-dimensional ultrasonic standing wave propagated in the vertical direction.

The second category of model pertains to the macroscopic scale of the entire suspension or emulsion. Here, the rates of collisions between individual pairs of particles (agglomeration or homogeneous coalescence) or between the particle and a surface within the acoustic field (particle deposition or heterogeneous coalescence) predicted by the microscopic model are used to forecast agglomeration or coalescence rates for the overall suspension. In addition, evolution of the particle size distribution driven by the ultrasonic standing wave field can be predicted. Experimental observations of the dynamics of the particle size distribution show good qualitative agreement with model predictions. Discrepancies between the experimental and modeling results are attributed to spatial non-uniformities in the acoustic field and the associated lateral radiation forces. The contribution of these forces to overall coalescence rates is described in terms of an effective strength of the ultrasonic field.

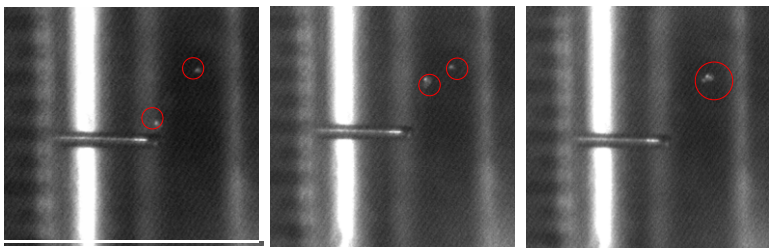

Fig. 1. Time series of ultrasonically driven coalescence of air bubbles in water.

Measurement of acoustic resonance line shapes by microbead acoustophoresis in straight microchannels

Rune Barnkob[1], Per Augustsson[2], Thomas Laurell[2], and Henrik Bruus[1]

[1]Department of Micro- and Nanotechnology
Technical University of Denmark
DTU Nanotech, Building 345 East
DK-2800 Kongens Lyngby, Denmark
Email: Rune.Barnkob@nanotech.dtu.dk
URL: www.nanotech.dtu.dk/microfluidics

[2]Division of Nanobiotechnology
Department of Electrical Measurements
Lund University
S-221 00 Lund, Sweden
Email: Per.Augustsson@elmat.lth.se

Introduction

Within the past five years there has been a significant increase in the number of novel applications of ultrasound standing waves for particle handling in microfluidic chips. In spite of this growing interest, detailed measurements of the resonance line shapes are lacking. We present such measurements based on tracking of individual polystyrene microbeads during acoustophoretic motion in straight water-filled microchannels in silicon/glass chips subject to piezo-induced ultrasonic pressure fields. From the measured line shapes we extract the corresponding Q factors and thus gain insight in the nature of the acoustic energy dissipation of such systems.

Experiment

We have fabricated microfluidic silicon/glass chips of different widths containing straight, 377-µm-wide channels, Fig. 1(a). In each experiment a chip was mounted on a piezoelectric transducer, and a dilute, aqueous suspension in the range from 0.01 g/mL to 0.05 g/mL of 5-µm-diameter polystyrene microbeads was injected into the microchannel, Fig. 1(b).

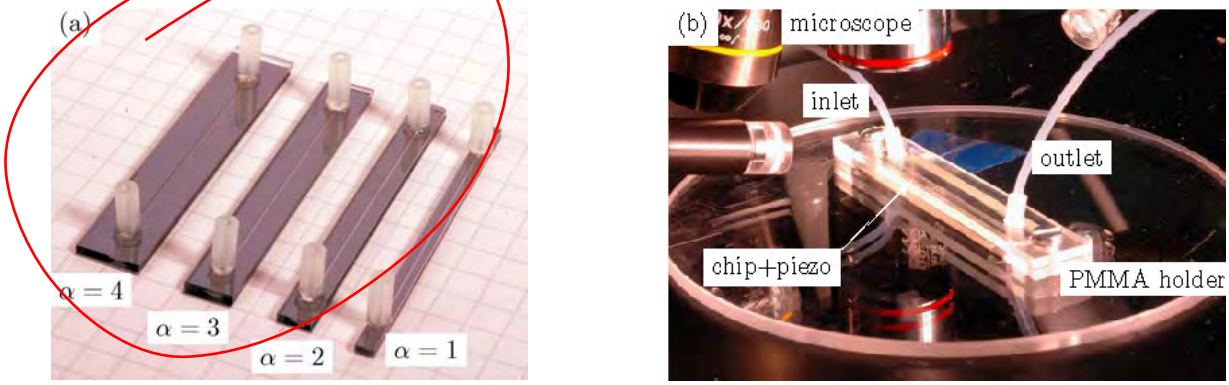

Fig. 1. (a) The silicon/glass chips containing straight channels of length l = 40 mm, width w = 0.377 mm, and height h = 0.157 mm. The channels are etched down into the silicon chip of thickness h_{si} = 0.35 mm, and they are covered by a pyrex lid of thickness h_{py} = 1.13 mm. The lengths of the chips are L = 50 mm and the widths are W = 2.5 mm (α = 1), W = 4.7 mm (α = 2), W = 6.8 mm (α = 3), and W = 9.0 mm (α = 4), respectively. (b) A photograph of the experimental setup with the chip and the PZT piezo crystal mounted under the microscope and the CCD camera. The piezo has the dimension 50.0 mm × 12.0 mm × 1.0 mm.

The acoustic energy density was measured by observing the transient, acoustophoretic motion of the microbeads. First, the driving frequency was tuned until observing a strong, resonant, acoustic focusing of the polystyrene microbeads towards the center of the channel. Then, the ultrasound field was turned off, and a fresh solution of microbeads was injected into the channel. When a homogeneous microbead distribution was observed, the flow was stopped. Finally, the ultrasound was turned back on, and the transient focusing of the microbeads towards the channel center was recorded by a CCD camera. Employing the free video analysis tool *Tracker 2.6* on the resulting

movie, we determined the transverse position y for a number of particles on each frame, for which the time t is known. The resulting lists of (t,y)-coordinates can be extracted for all tracked microbead paths at any given driving frequency f and driving voltage U_{pp}.

Results

Using the standard theory for acoustophoresis we have obtained an analytical expression for the particle path $y(t)$ containing the acoustic energy density E_{ac} as an unknown parameter [1]. This expression is fitted to the measured data points (t,y), and E_{ac} is extracted. In Fig. 2(a) we have plotted E_{ac} versus the driving frequency f and fitted the obtained resonance peaks by the sum of two Lorentzian line shapes. The two observed peaks, differing Δf = 9.4 kHz in resonance frequency, correspond to two resonances. The high-f resonance has one more axial pressure node than the low-f resonance as illustrated by the pressure field simulation in Fig. 2(b). From the Lorentzian line shapes we obtain the Q factors of the resonance peaks to be 209 and 577, respectively. In the case of having only viscous dissipation we expect the Q factors to be Q ≈ 10^4, which implies that the observed resonance widths are mainly due to the acoustic coupling to the surroundings.

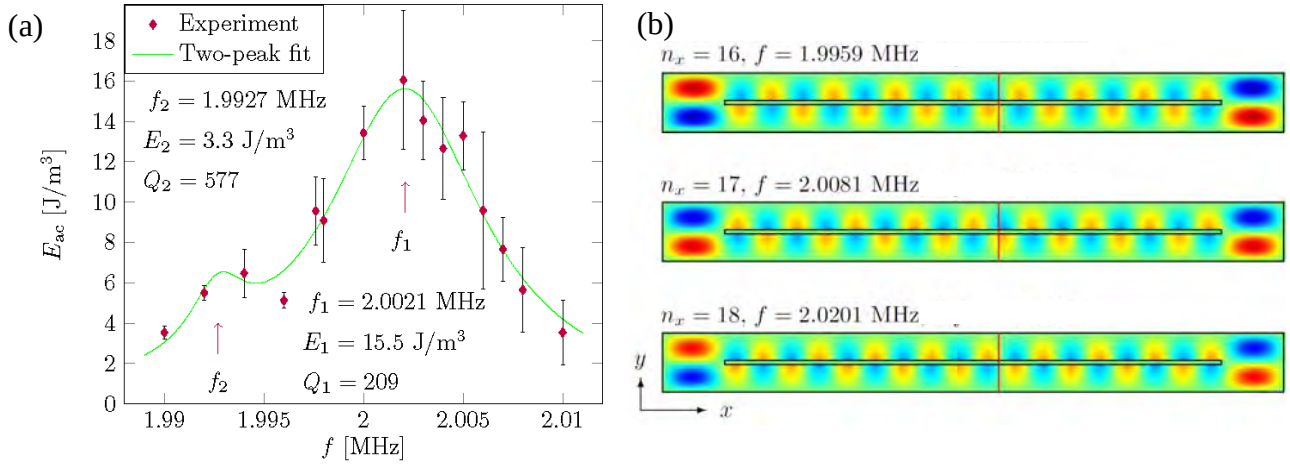

Fig. 2. (a) Measured acoustic energy density E_{ac} versus applied frequency f on the piezo transducer (points) for α = 2. A sum of two Lorentzian peaks (full line) fits the data reasonably well. (b) Top-view colorplots of the pressure (blue negative, red positive) for three ultrasound resonances calculated in a simplified 2D model [2]. For each resonance is shown the number of n_x of pressure nodes in the axial direction and the resonance frequency f. The two resonances are separated by $\Delta f \approx 12$ kHz.

Conclusion

We have measured the acoustophoretic motion of microbeads in dilute, aqueous solutions in straight, water-filled channels in silicon/glass chips subject to piezo-induced ultrasound standing waves. For a given driving frequency and voltage amplitude of the piezo transducer, microbead paths have been recorded by a CCD camera and fitted to a theoretical curve. From the curve fit we have obtained the acoustic energy density. Furthermore, by plotting the energy densities as a function of the applied ultrasound frequency, we obtained Lorentzian line shapes, from which we can determine precise values of the resonance frequency and the Q factor for each acoustic resonance. This novel technique opens up for a detailed, *in-situ* study of microchannel acoustophoresis and its energy-loss mechanisms [3].

References

[1] H. Bruus, *Theoretical Microfluidics*, Oxford University Press (Oxford, 2008).

[2] R. Barnkob and H. Bruus, *Acoustofluidics*: *theory and simulation of radiation forces at ultrasound resonances in microfluidic devices*, Proceedings of Meetings on Acoustics **6**, 020001 (2007), 157th Meeting Acoustical Society of America.

[3] R. Barnkob, P. Augustsson, T. Laurell, and H. Bruus, *Measuring the local pressure amplitude in microchannel acoustophoresis*, Lab Chip (submitted 2009).

A thin-reflector mode for ultrasonic particle manipulation in layered resonators

Peter Glynne-Jones[1], Rosie Boltryk[1], Nick Harris[2], Martyn Hill[1]

[1]School of Engineering Sciences
University of Southampton
Southampton
P.Glynne-Jones@soton.ac.uk

[2] Electronics and Computer Science
University of Southampton
Southampton

Background:

Previous literature has described two major classes of planar acoustic particle manipulation devices: (a) those in which the dominant resonance is in the fluid layer, leading to agglomeration at one or more pressure nodes within the fluid layer; and (b) those in which a resonant reflector layer provides a pressure release boundary condition, causing the agglomeration position to occur at a pressure node close to the fluid/ reflector interface (quarter-wave devices)

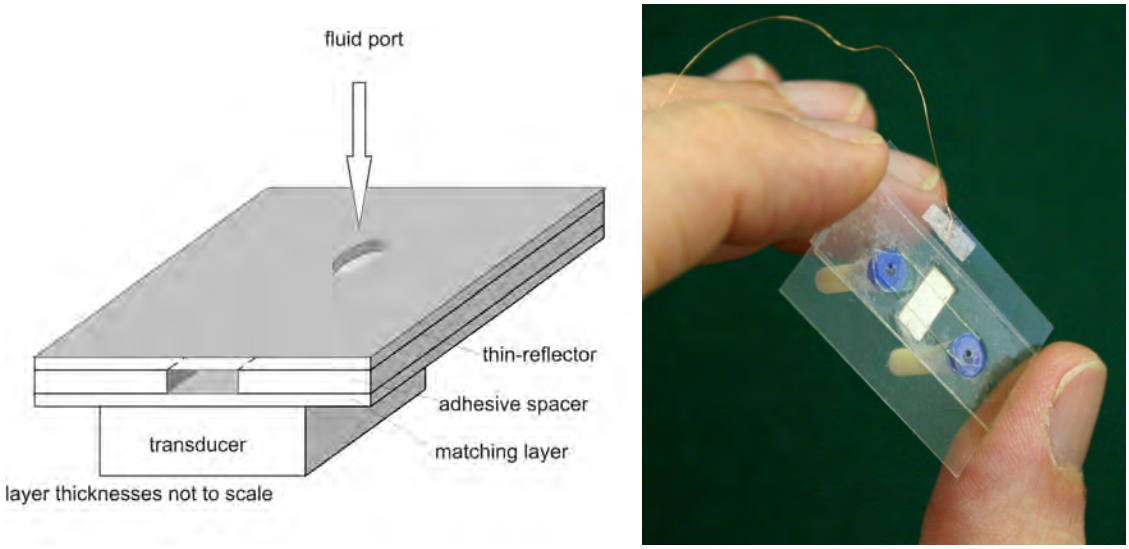

Fig. 1. Cut away diagram of device, and photograph.

Methods & Results:

We describe here a new arrangement which operates at the first thickness resonance of a composite structure (fig.1), with energy distributed across all layers of the device as shown in fig. 2. This leads to pressure nodes at the air boundaries of a device. By designing with only a thin reflector layer (a thickness of ~λ/15 in this case) particles at all positions within the channel are forced to the reflector/fluid layer boundary.

We model and experimentally characterise a device, and show that it can produces forces of order 50pN on a 10µm diameter polystyrene bead with transducer excitation of 25Vpp. We demonstrate that this configuration will work efficiently with lossy polymer reflector layers, and further show that by incorporating an additional thin plastic layer between the transducer and fluid layers it is possible to create a disposable sample cuvette that is easily mounted within a device.

Conclusions:

The advantages of this arrangement are energetic acoustic modes, thin device walls compatible with high numerical aperture microscope objectives, and the possibility of creating cheap, disposable sample cuvettes. The design is also more stable than quarter-wave devices to small variations in chamber dimensions. We foresee this having applications in bio-sensing, cell handling and fractionation devices.

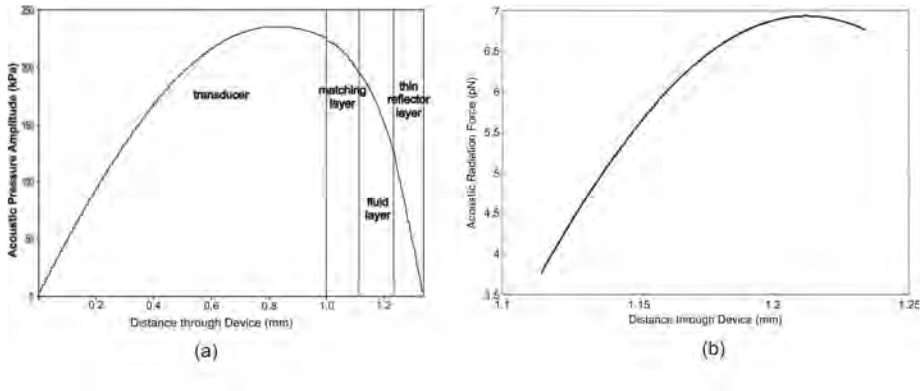

Fig. 2. Acoustic field distribution and radiation force in example device.

Calculations for the time-averaged acoustic forces and torques experienced by a rigid cylinder in a slightly viscous fluid

Jingtao Wang, Jurg Dual

Institute of Mechanical Systems
Dept. of Mechanical and Process Eng.
ETH Zurich
CH-8092 Zurich
Switzerland
wang@imes.mavt.ethz.ch

One of the most important applications of time-averaged acoustic forces is contactless particle manipulation. It is necessary to accurately predict the actual acoustic forces acting on suspended particles in a real fluid to design ultrasonic particle manipulators. Previous theoretical and numerical calculations on this topic mainly concentrated on an ideal fluid. In this paper, the time-averaged acoustic forces and torques experienced by a rigid circular cylinder in a slightly viscous fluid under one or two orthogonal standing acoustic waves are investigated in detail by analytical formulations and numerical simulations. The analytical solutions are derived from Nyborg's [1] theoretical calculations of acoustic streaming near boundaries. Simplified solutions are also obtained under the limited condition that the wave length is much greater than the cylinder radius. The numerical simulations are carried out by solving the full N-S equations based on the finite volume method (FVM) and the perfectly matched layer (PML) technique used in our previous paper [2]. The acoustic boundary layer is described in detail by introducing a large number of very thin elements near the cylinder surface. Fig. 1 (a) demonstrates a typical mesh and distribution of pressure at 200 cycles for two orthogonal waves, where the cylinder radius is 60, the wave length is 1000, and the ratio of the thickness of boundary layer to the cylinder radius is about 0.04. Fig. 1 (b) shows the detailed mesh configuration near the cylinder surface.

The numerical results agree well with those from the analytical formulation. Some conclusions can be made as follows. Generally speaking, in the cases of one standing wave, the total mean time-averaged forces are a little larger than those calculated without viscosity when the particle is much smaller than the wave length, and there is also no torque acting on the cylinder as in an ideal fluid. In the case of two orthogonal standing waves, an extra torque acting on the cylinder is observed under the condition that the phase difference between the two waves is not equal to zero. This phenomenon can be used to generate continuous rotation of a particle.

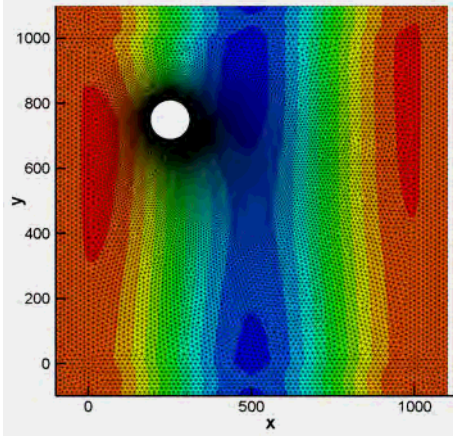

Fig. 1 (a) mesh and pressure contours at 200*T*??

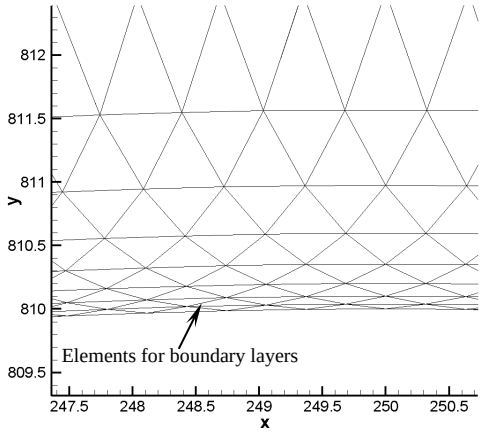

Fig. 1 (b) mesh near the cylinder surface

References

[1] W. L. Nyborg, the Journal of the acoustical society of america, 1958, 30(4), 329
[2] J. Wang, J. Dual, Journal of Physics A, 2009, 42, No. 285502

Some biological applications of Ultrasound Standing Wave Systems

Despina Bazou[1]

[1]CRANN
Trinity College Dublin
Dublin 2, Dublin
Ireland
Bazoud@tcd.ie

[2]Pharmacology Department
Trinity College Dublin Trinity
Dublin 2, Dublin
Ireland

[3]Smurfit Insitute of Genetics
College Dublin
Dublin 2, Dublin
Ireland

Investigation of cancer cell/platelet interactions in an ultrasound trap

Maria-Jose Santos Martinez[2], Carlos Medina[2], Marek Radomski[2]

Platelets play an integral role in the haematogenous spread of cancerous cells during the metastatic cascade. When cancer cells (*i.e.* a tumour) are covered with a coat of platelets they acquire the ability to invade the body's immune system. Indeed, it has been shown that platelets protect tumours from tumour necrosis factor α-mediated cytotoxicity and also they release a number of growth factors that can be used by cancer cells for growth. In this project we aim to investigate tumour cell-induced platelet aggregation (TCIPA) as well as to pharmacologically manipulate this interaction in suspension. An ultrasound trap[1] is used to drive, by acoustic radiation force, cells to a pressure node plane and then concentrate them within that plane into a 2-D aggregate within 60 s. The aggregation process is microscopically observed and video recorded through the glass reflector of the ultrasound resonator.
An aggregate of colon or ovarian cancer cells was allowed to be formed in the ultrasound trap for 10 min (Fig. 1a). Human platelets were then perfused at a flow rate of 3 µl/min; the cancer cell aggregate was fully 'encapsulated' by platelets (Fig. 1b). The interaction was continuously monitored for up to 15 min. It was shown that upon platelet activation, the aggregate disrupts (Fig. 1c). Pharmacological manipulation of this interaction revealed that prostacyclin is the most potent inhibitor of platelet activation; phenanthroline comes next while aspirin is ineffective. This is a novel mechanism that has not been previously reported and has a major impact on the metastasis mechanism, as parts of the tumour can be then transported through the hematopoietic system to various organs.

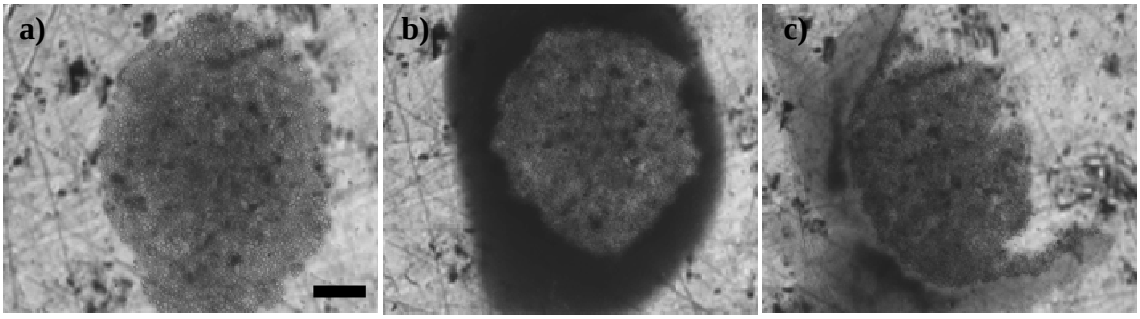

Fig. 1. a) 2-D aggregate of colon cancer cells levitated in the ultrasound trap for 10 min, b) human platelets were perfused and encapsulated the aggregate, c) aggregate disruption following platelet activation. Scale bar is 100 µm

Gene expression analysis following levitation of embryonic stem cells in an ultrasound trap

Roisin Kearny[3], *Fiona Mansergh*[3], *Michael Wride*[3]

Embryonic stem (ES) cells hold great promise as a potential source for cell-based therapeutic strategies owing to their intrinsic ability to self-renew (pluripotency) and differentiate into functional cell types[2]. This is reflected *in vitro* through formation of embryoid bodies (EBs). The ability to rapidly and reproducibly generate EBs of the same size can help understand the mechanisms controlling stem cell differentiation, a key to future advances in tissue and organ regeneration. Here, the ultrasound trap provides means to rapidly generate 3-D cell aggregates in suspension (*i.e.* EBs). The genetic profile of the 'ultrasound-formed' EBs is assessed with particular attention to the suitability of the ultrasound system to stem cell manipulation.

RNA was isolated from embryonic stem cells and EBs, following levitation in the ultrasound trap for 5 and 60 min and for different acoustic pressure amplitudes (0.85 and 0.06 MPa). An initial screen was carried out to test for differences in the gene expression of various pluripotency and early development markers such as: Nodal, Kdr, Fgf5, Gsc, Brachyury, Oct4, Nanog, Rex 1, Nestin, for neuronal, glial and eye development: Mash1, Dcx, Chx10, Otx2, Pax6, Mitf, Crx, and Nrl, using semi-quantitative RT-PCR. The results suggested that there is no effect on stem cell differentiation even of the 'strongest' employed ultrasound field (2.2 MHz, 0.85 MPa, 60 min of operation). Further experiments were carried out using real-time PCR (qPCR) to validate the RT-PCR observations. Immunofluorescence and western blotting analysis further confirmed the above results, *i.e.* the respective proteins were expressed and no difference could be detected in the immunostaining pattern between control and treated EBs. These results have provided important insights into stem cell differentiation and pluripotency that are relevant to developing stem cell therapies and tissue/organ regeneration but also further confirm the safety of medical ultrasound.

[1] Bazou D et al. (2005) Mol. Membr. Biol. 22 (3): 229 - 240
[2] Mansergh FC et al. (2009) BMC Dev. Biol. 9: 9 – 26

Bio-suspensions in the ultrasonic h-shape filter

Cosima Koch[1], Stefan Radel[1,2], Ewald Benes[1]

[1]Vienna University of Technology
Institue for General Physics
Wiedner Hauptstraße 8-10/134
1040 Wien
Austria
cosima.koch@tuwien.ac.at

[2]Vienna University of Technology
Institute of Chemical Technologies and Analytics
Getreidemarkt 9/164
1060 Wien
Austria
stefan.radel@tuwien.ac.at

The ultrasonic h-shape filter (Figure 1) was used for the separation of suspensions of the yeast *Saccharomyces cerevisiae*. The filter works as follows: when the yeast cell suspension enters the resonator through the inlet, the yeast cells are held in the pressure nodal planes which act like rails and guide the cells the outlet in the lower part of the resonator. An enriched phase, i.e. a suspension with higher cell concentration than the suspension entering the filter, can be collected from that outlet, while a cleared phase, i.e. a suspension with lower cell concentration compared to the suspension entering the filter, can be collected from the top outlet. The separation efficiency of the filter, i.e. the ability to retain suspended yeast cells, was assessed. To examine the influence of the separation process on the cells, cell viability by methylene blue counts, possible cell rupture assessed by the protein concentration of the supernatant and growth were investigated before and after sonication.

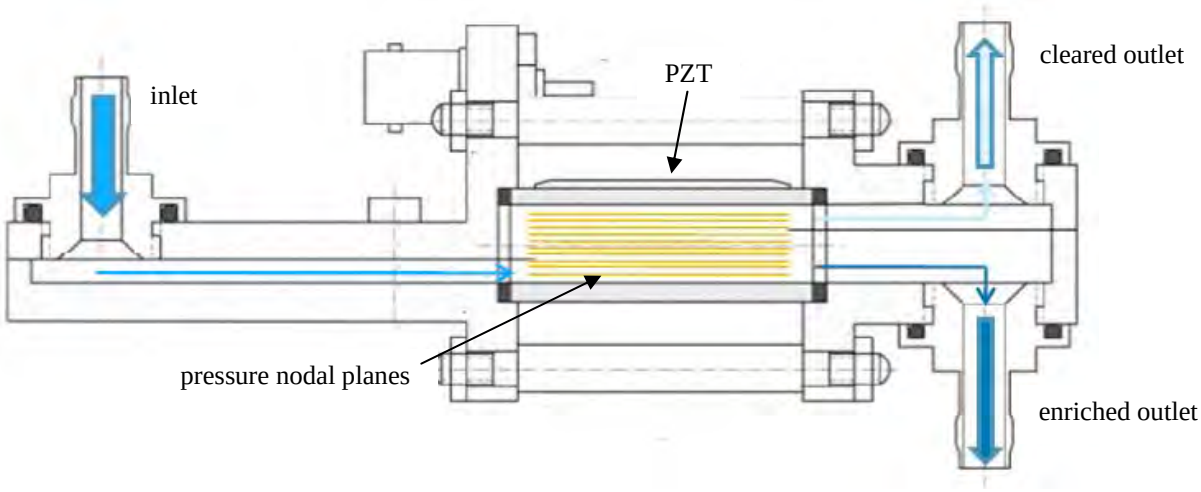

Figure 1: Schematic view of the h-shape filter.

The filter was operated at a frequency of 2.1MHz at a power input of 3W true electrical power input. The filter was shown to work well for cultured yeast suspended in Malt Extract Broth, for which a separation efficiency of 89+/-6% was found. Wet yeast suspended in phosphate buffered saline (PBS, 0.9% NaCl), PBS 2x (1.8% NaCl) and H_2O tap was not retained as efficiently.

For all the suspensions cell viability was not affected by sonication, remaining at high levels. However, in two cases when cultured cells suspended in Malt Extract Broth were driven through the resonator, a significant decrease of cell viability of the sonicated cells was measured. Cell concentration of retentate samples of cultured yeast/Malt Extract Broth-suspensions was 20% higher for counts 18 hours after sonication than that of counts immediately after sonication (99% significance, 2-sided t-test). For control groups and the filtrate samples no such increase was detected. Cell leakage caused by the separation process was detected by a significant increase in UV O.D. for cells suspended in PBS. For PBS 2x- and H_2O tap-suspensions no significant difference in UV O.D. between control and sonicated groups, respectively, was found.

Prolonged ultrasonic trapping and characterization of living cells in a microfluidic chip

Ida Iranmanesh, Jessica Svennebring and Martin Wiklund

Royal Institute of Technology
Dept. of Applied Physics
KTH - Albanova
SE-106 91 Stockholm
Sweden
martin@biox.kth.se

Ultrasonic manipulation in microfluidic chips is a promising method for gentle handling of cells or other bioparticles. We have previously demonstrated proliferation of cells after they have been trapped in a chip for up to 75 min of ultrasound exposure [1]. We have also demonstrated how to control the temperature in the flow channel for long exposure times (up to 12 hours) [2]. In this abstract, we investigate the viability *in situ* of cells trapped in a microfluidic chip as a function of actuation voltage and exposure time.

The device is depicted in Fig. 1. It consists of a glass-silicon-glass stack and a wedge transducer operating at 6.9 MHz. The microchannel has an ultrasonic cage designed as a confocal resonator, see Fig. 1. The cells employed in the experiments were human Epstein-Barr virus (EBV)-transformed B cells labelled with green-fluorescent calcein-AM (live cell indicator) and red-fluorescent propodium iodide (dead cell indicator).

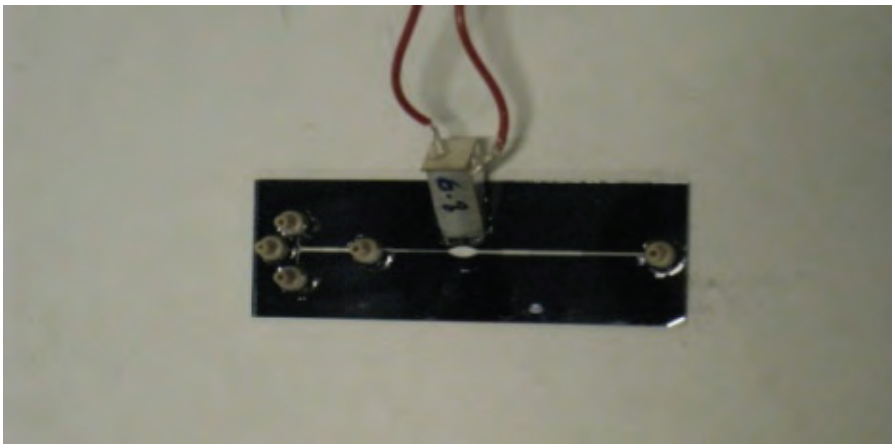

Fig. 1 The chip with a mounted wedge transducer.

Two different parameters were investigated: Exposure time and actuation voltage. In the first experiment, trapped cells were monitored every 30 min for up to 5 hours during 10 V_{pp} actuation voltage (see Fig. 2). In the second experiment, trapped cells were monitored while increasing the actuation voltage from 10 to 25 V_{pp} in steps of 5 V_{pp} (see Fig. 3). This voltage interval was chosen in order to measure the immediate effect on the viability for excess voltage levels beyond the standard operating level of 10 V_{pp}. Both experiments were performed without any fluid flow.

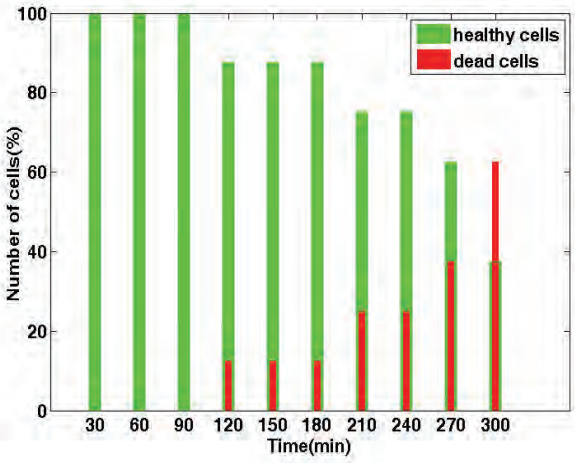

Fig. 2. Cell viability as a function of exposure time.

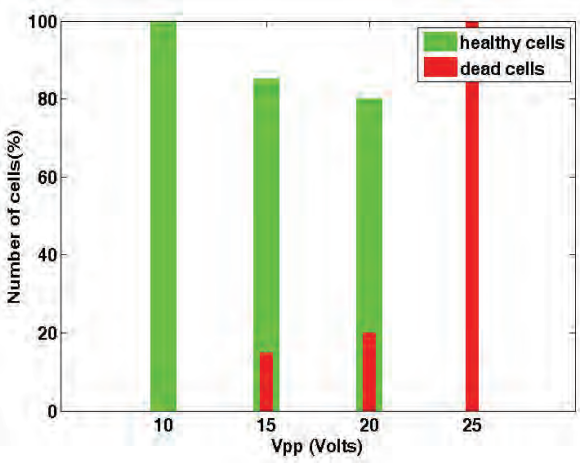

Fig. 3. Cell viability as a function of actuation voltage.

The measurements suggest that cells may stay viable for up to 5 hours in our system during continuous ultrasonic exposure at 10 V_{pp} actuation voltage (see Fig. 2). At even higher actuation voltages, cell death may occur immediately (see Fig. 3). We believe the major reasons for the cell death are the lack of CO_2 control for long-term exposure at medium voltages (cf. Fig. 2), and heating for short-term exposure at high voltages (cf. Fig. 3). Future improvements are expected if the system is operated in perfusion mode with continuous exchange of CO_2 and temperature-regulated cell medium.

References:

[1] J. Hultström, O. Manneberg, K. Dopf, H. M. Hertz, H. Brismar and M. Wiklund, Ultrasound Med. Biol. **33**, 145 (2007).

[2] J. Svennebring, O. Manneberg and M. Wiklund, J. Micromech. Microeng. **17**, 2469 (2007).

Ultrasonic manipulation in microfluidic systems: Selective cell handling and characterization

Jessica Svennebring, Otto Manneberg, Ida Iranmanesh, Hans M. Hertz and Martin Wiklund

Royal Institute of Technology
Dept. of Applied Physics
KTH - Albanova
SE-106 91 Stockholm
Sweden
martin@biox.kth.se

In the present abstract, we review our activities in ultrasonic manipulation for dynamic live cell imaging. The system is based on multiple-frequency ultrasonic actuation of a microfluidic chip made of silicon and glass [1]. Combined with state-of-the-art optical microscopy, the device is suitable for high-resolution dynamic characterization of live cells.

First, we investigate viability and proliferation of adherent COS-7 cells exposed to long-term ultrasound in a temperature-regulated microfluidic chip by a combination of several indicators of the cell state, e.g., fluorescence assays and automatic image analysis, see Fig. 1. No deviations in the doubling time from expected values for adherent cells (24-48 h) were observed for COS-7 cells trapped at acoustic pressure amplitudes up to 0.85 MPa, and for trapping times up to 75 minutes. The results demonstrate the potential of ultrasonic standing waves as a tool for gentle and long-term manipulation of low cell numbers in microfluidic systems [2].

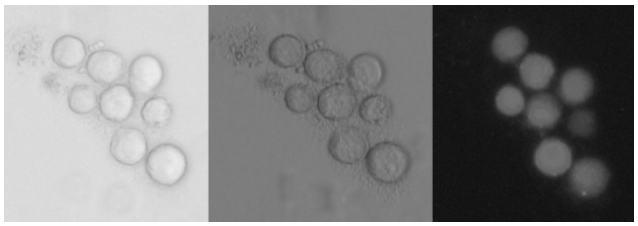

Fig. 1. Ultrasonically trapped cells (~10 µm) imaged using bright field, phase contrast and fluorescence microscopy.

In order to achieve a constant physiological temperature inside the chip, one approach is to use external heating. However, heat is also generated in the transducer which increases the local temperature in the microchannel. Therefore, we have designed a temperature regulation system based on ultrasound-generated heating in combination with a heatable mounting frame for the chip to accurately control the temperature independently of both the acoustic pressure amplitude and the flow rate. Calibration data (the temperature increase as a function of the transducer voltage) is used for defining the mounting frame temperature. The system can handle small sample volumes (<1 µl) for manipulation of individual cells with a regulation accuracy of the order of ±0.1°C [3].

We also demonstrate selective retention and positioning of cells or other bioparticles by ultrasonic manipulation in a microfluidic expansion chamber during microfluidic perfusion [4]. The chamber is designed as a confocal ultrasonic resonator for maximum confinement of the ultrasonic force field at the chamber center, where the cells are trapped. By triple-frequency ultrasonic actuation during continuous microfluidic sample feeding, a set of several manipulation functions performed in series is demonstrated: sample bypass—injection—aggregation and retention—positioning. This device can be

used for real-time high-resolution characterization of a controlled number of cells retained in a continuous-flow perfusion system.

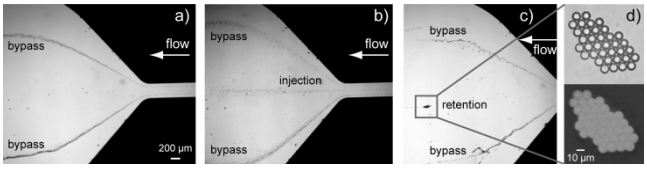

Fig. 2. Selective retention and positioning from a continuous sample flow (5 µL/min) containing 10 µm fluorescent beads: (a) sample bypass (b) sample injection and bypass (c) sample retention and (d) retained bead aggregates.

REFERENCES

[1] O. Manneberg, J. Svennebring, H.M. Hertz, M. Wiklund,"Wedge transducer design for two-dimensional ultrasonic manipulation in a microfluidic chip" *J. Micromech. Microeng.*, vol 18,pp. 095025-34, 2008

[2] J. Hultström, O. Manneberg, K. Dopf, H.M. Hertz, H. Brismar, M. Wiklund, "Proliferation and viability of adherent cells manipulated by standing-wave ultrasound in a microfluidic chip" *Ultrasound Med. Biol.*, vol. 33, pp.145–151, 2007

[3] J. Svennebring, O. Manneberg, M. Wiklund, "Temperature regulation during ultrasonic manipulation for long-term cell handling in a microfluidic chip", *J. Micromech. Microeng.* , vol. 17,pp. 2469–2474, 2007

[4] J. Svennebring, O. Manneberg, P. Skafte-Pedersen, H. Bruus, M. Wiklund, " Selective bioparticle retention and characterization in a chip-integrated confocal ultrasonic cavity", *Biotechnol. Bioeng*., vol. 103, pp. 323-328, 2009

Highly parallelized cell aggregation by ultrasound for studies of immune cell interaction

Bruno Vanherberghen, Otto Manneberg, Athanasia Christakou, Thomas Frisk, Björn Önfelt and Martin Wiklund

Royal Institute of Technology
Dept. of Applied Physics
KTH - Albanova
SE-106 91 Stockholm
Sweden
martin@biox.kth.se

We have previously demonstrated ultrasonic "micro-caging" in 3D of individual cells for high-resolution optical live cell imaging [1]. We here present a parallelization of the micro-cage concept in a chip with 100 micro-wells employing ultrasonic resonances stabilized by frequency modulation to achieve parallel formation of bead or cell clusters. The goal is to use the device for high-resolution screening of cell aggregates, in order to elucidate individual immune cell interactions.

The device consists of a 500 µm thick silicon wafer of 22×22 mm^2, with 100 wells in the form of filleted squares (side length 300 µm) separated by 100 µm walls, bonded onto coverslip-thickness glass and actuated using a wedge transducer of a 45° angle (Fig1). The transducer is operated around 2.5 MHz in sawtooth-shaped linear sweeps at a rate of 1 kHz and bandwidth ~100 kHz. The cell sample is loaded from above and stored in a PDMS gasket. The transducer – chip device is placed in a confocal microscope (Zeiss LSM 510 Meta) equipped with a temperature- and CO_2-regulated climate chamber.

Fig 1. Schematic of the chip (left) and a photo of the chip with a mounted transducer and PDMS gasket (right).

While ultrasonic particle arraying has been demonstrated previously [2-4], it has been performed in closed systems apart from inlet and outlet channels and thus require further microfluidic equipment such as tubing and pumps to load the systems. Our device is an open multi-well system ensuring similar chemical and physical environments. Furthermore, in contrast to Refs. 2-4, our device does not employ a multiple-node large chamber. Instead, we have a single trapping position/node in each well, which makes it possible to turn off the ultrasound without the risk of cross-contamination between the cell aggregates. This is particularly important for the relatively mobile immune cells studied.

Importantly, our system was both robust and gentle. Long term exposure of human tumor lymphocytes to continuous ultrasound (>72hrs) did not significantly affect their long term viability, with the majority

proliferating several times, while remaining selectively retained within the center of the individual wells.

By seeding Natural Killer (NK) cells and target cells together we were able to observe many individual immune cell interactions in parallel with both low resolution and high resolution imaging. The trapping efficiency of the device, measured as the relative amount of cells that were merge in clusters, was found to be 95.3±1.8%. A typical tile scan from such an experiment is shown in Fig. 2.

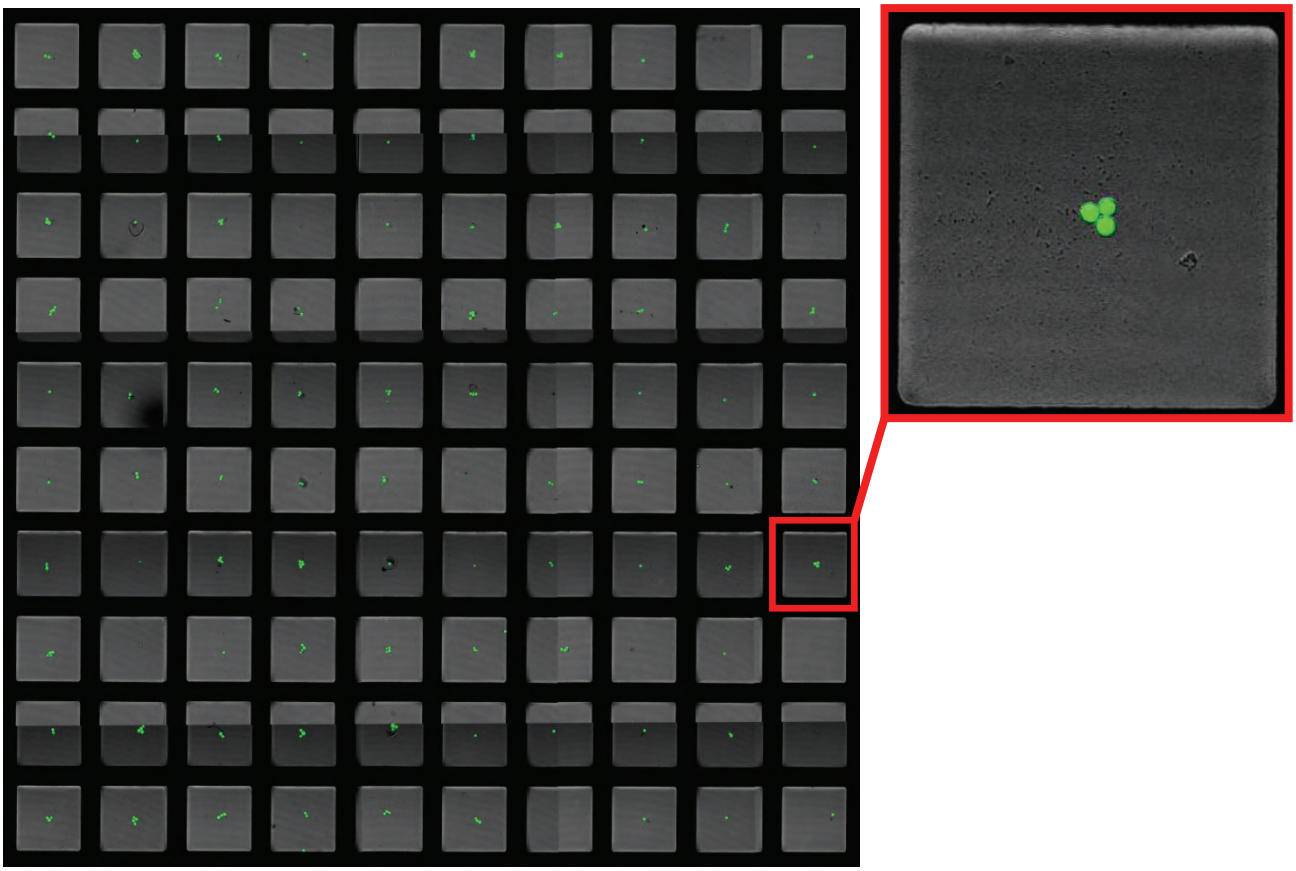

Fig 2. Tile scan in the confocal microscope of all 100 wells of the microchip and an insert of a single well with calcein labelled tumor lymphocytes trapped in the center of the wells.

References:

[1] O. Manneberg, B. Vanherberghen, J. Svennebring, H. M. Hertz, B. Önfelt and M. Wiklund, Appl. Phys. Lett. **93**, 063901 (2008).

[2] T. Lilliehorn, U. Simu, M. Nilsson, M. Almqvist, T. Stepinski, T. Laurell, J. Nilsson, S. Johansson, Ultrasonics **43**, 293 (2005).

[3] A. Haake, A. Neild, G. Radziwill and J. Dual, Biotechnol. Bioeng. **92**, 8 (2005).

[4] J. Shi, D. Ahmed, X. Mao, S.-C. Steven Lin, A. Lawita and T. Jun Huang, Lab Chip **9**, 2890 (2009).

USW manipulating the location of suspended yeast cells in close proximity to an in-line infrared spectroscopy probe

Stefan Radel[1], Markus Brandstetter[2], Bernhard Lendl[2]

[1]Vienna University of Technology
Inst. of Applied Physics
Wiedner Hautptstr. 8-10/134
A-1040 Wien
Austria
stefan.radel@tuwien.ac.at

[2]Vienna University of Technology
Inst. of Chemical Technologies and Analytics
Getreidemarkt 9/164
A-1060 Wien
Austria

The growing use of biotechnology as a manufacturing route for e.g. antibiotics and other medical compounds stimulates the development of reliable sensors for bioprocess purposes. Vibrational spectroscopy is an optical measurement technique increasingly popular in process analytical chemistry because of its ability to directly provide molecular specific (bio-)chemical information about a given sample. The ATR (Attenuated Total Reflection) spectroscopy is a widely used method for mid-infrared vibrational spectroscopy especially in connection with highly absorbing samples like e.g. aqueous solutions. Only a thin film of some micrometers in the proximity of the ATR sensitive element is spectroscopically analyzed, beyond this evanescent field the instrument is “blind”. This opens the possibility to employ the radiation forces within an USW to manipulate the whereabouts of suspended particles – biological cells in the case of a bioreactor - relative to the ATR. More precisely the field is used to either push the particles towards the optical sensor or away from it. This enables one to detect the infrared spectrum of cells and the supernatant independently.

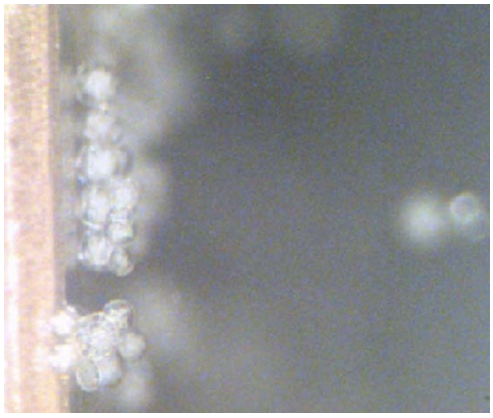

Fig. 1. Resin beads suspended in methanol being pushed to a brass dummy probe acting as a reflector for the USW.

Light micrographs (Fig.1) suggested, that the task was successfully accomplished with polystyrene beads suspended in methanol, aggregates were manipulated to and from the reflector of an ultrasonic resonator. Feasibility was confirmed by infrared absorption spectra recorded when PTFE particles suspended in tetrahydrofuran were manipulated in the evanescent field of a truncated, cone-shaped ATR tip[1].

Two key factors are of great importance when bioprocess monitoring and control is in the focus of attention. Firstly, the time resolution of a measurement system has to be sufficiently higher than the

[1] Radel et al. *Observation of particles manipulated by ultrasound in close proximity to a cone-shaped infrared spectroscopy probe.* Ultrasonics (2009), in press, doi:10.1016/j.ultras.2009.09.030

generation time of the observed microorganism. Secondly, the delivered information necessarily has to reflect the condition of the suspension within the bioreactor as close as possible.

We have recently reported the successful application of an USW within an on-line ATR flow cell[2]. The USW was employed to increase the settling speed of the cells, an infrared spectrum of the culture could be obtained in approx. 70 seconds, this meant an acceleration by a factor of 2.5. Infrared spectra in this set-up were taken on-line in bypass to the bioreactor, resulting in a possibility of a slight temperature shift and the risk of contamination.

In the present work we set out to develop a robust, fast *in-line* sensor delivering chemical information of the particles and the liquid of a suspension combining the two technologies.

The device was constructed to be inserted into a standard port of a bioreactor, hence the environment during measurement shall be guaranteed to be unaltered. Moreover, due to the high cell concentration that can be established in seconds in the evanescent field of the ATR by the USW, fast response times were warranted. A novel industrial fibre-optic probe with a flat ATR element was used, as this element constituted the reflector of the ultrasonic resonator (see Fig.2).

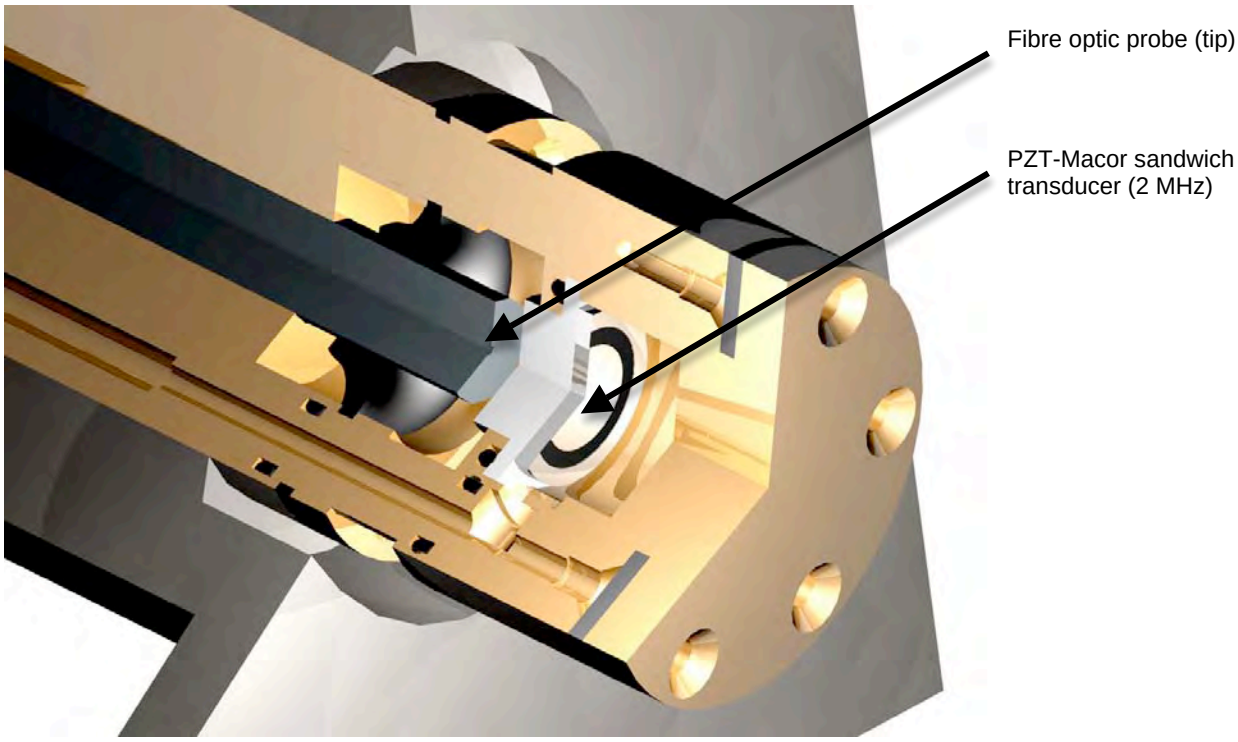

Fig. 2. Tip of the prototype of an in-line ATR probe exploiting an USW to actively control the spatial residue of biological cells in suspension.

Infrared spectra showing an USW populating and depopulating the sensitive zone of the ATR will be presented. It was possible to assess a yeast culture independently from its supernatant. Measurements showed lower absorption when compared to results of wet sediments (which cannot be produced within a bioreactor). Infrared spectra of the culture in suspension were measured within some ten seconds, no contamination of the ATR was observed.

[2] Radel et al. *Ultrasonic particle manipulation exploited in on-line infrared spectroscopy of (cell) suspensions.* Elektrotech. Inftech. (2008) vol. 125 (3) pp. 76-81, doi:10.1007/s00502-008-0514-3

Cell trapping in single-use capillaries with MALDI-MS readout

Björn Hammarström[1], Thomas Laurell[1], Mikael Evander, Johan Nilsson[1] and Simon Ekström[1]

[1]Lund University
Dept. Electrical Measurements
Box 118
SE-221 00 Lund
Sweden
bjorn.hammarstrom@elmat.lth.se

Technology that enables investigation of cell-cell or cell-ligand interactions on small populations of cells with high sensitivity, specificity and reproducibility has numerous high-impact applications in life science and drug discovery. With this in mind, a novel acoustic trapping technique using borosilicate capillaries has been developed and integrated with mass spectrometric analysis (MS). This has been applied for analysis of red blood cells (RBC).
To facilitate acoustic trapping a rectangular borosilicate capillary is laminated with a miniature ultrasonic transducer (size:…..). Due to attenuation in the capillary the acoustic field is confined to the area immediately above the transducer. The localized field is capable of retaining cells or particles against fluid flow in a non-contact fashion. For this system, 2000x200 µm capillaries were used and actuated at 7.5 MHz to provide reproducible double-node trapping. With this microfabrication-free approach to acoustic trapping the capillaries could easily be exchanged between each trapping event eliminating the risk of cross-contamination.

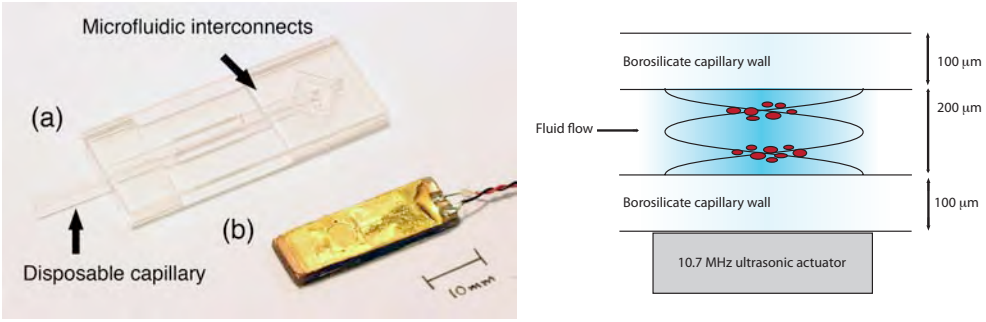

Fig. 1. Left, single-use rectangular trapping capillary mounted in PMMA holder (a) and actuation chip holding the ultrasonic actuator. Right, cross-section illustrating double-node trapping of RBC.

The trapping capillary and holder was mounted on a XYZ-stage allowing aspiration of multiple samples and deposition of perfusing liquids onto the wells of an ISET-plate[1] for reversed-phased SPE prior to MALDI-MS analysis. This set-up allows for analysis of sample fractions taken at different intervals to monitor any sequential treatment of the trapped bead/cell agglomerate.

[1] S. Ekstrom, L. Wallman, D. Hok, G. Marko-Varga, T. Laurell, J. Proteome Res., 5 (2006) 1071.

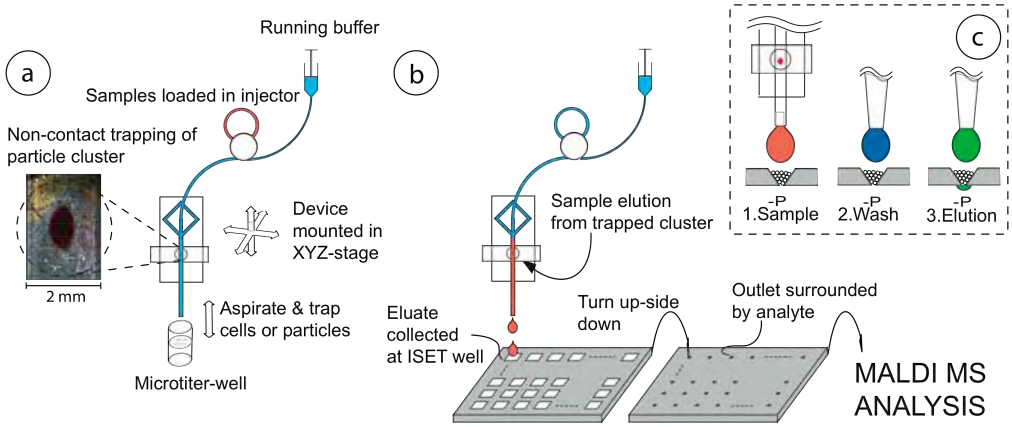

Fig. 2. Full system schematic, the capillary is mounted on a XYZ-stage allowing aspiration and deposition of multiple samples. Sample fractions for MS analysis are deposited directly onto an ISET plate for solid phase extraction prior to MS analysis.

Figure 3 shows the analytical read-out after MALDI-MS analysis of blood cells using the described system. A small blood sample was diluted with PBS and spiked with a drug compound and a peptide followed by incubation. 10 µL of this sample was aspirated into the capillary, trapping a cell agglomerate consisting of approx. 500 000 RBC (calculated from optical images). The trapped cells were washed through perfusion with running buffer (PBS), removing non-trapped cells and plasma. Subsequently the trapped RBCs were lysed through aspiration of 25 µL RBC lysis buffer. The perfusing wash and lysis solutions were collected as fractions on the ISET and MALDI analysis performed. The data, figure 3, confirms the expected results as the spiked drug could penetrate the RBC membrane and be observed in the lysed sample (***A3***), but not in the preceding wash (***A2***). The spiked peptide that should not be able to penetrate the RBC membrane could not be found in the lysed sample (**C3**). There were also many differentially observed peaks in the spectra, see enlargement ***B1-B3*** in figure 3.

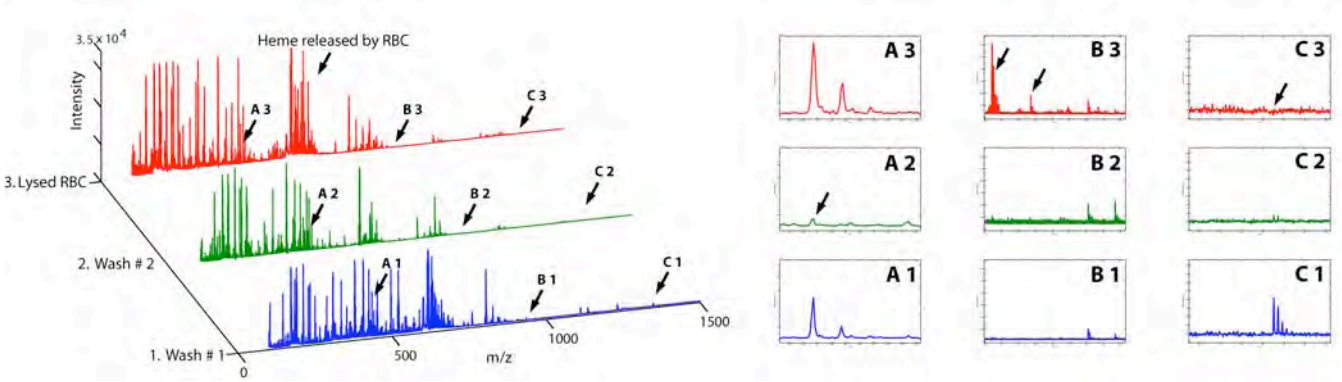

Fig. 3. Resulting mass-spectra after acoustic trapping and ISET sample preparation of approx. 500 000 RBC, arrows **A, B, C** indicates areas of interest that are enlarged in the left part of the figure. Wash number 1 (blue trace) contains the most of the un-trapped cells, debris and plasma. Wash number 2 (green trace) contains traces of plasma, surface bound species and cellular leakage. Lysis spectra (red trace) show the contents of the trapped RBC. Successful lysis is confirmed by the strong increase of signals from released Heme groups observed just above 600Da. Enlargement **A1-3** show the permeability of the spiked Drug. The disappearance in wash 2 and reappearance in the lysed sample confirms cell permeability of the drug. Enlargement **B1-3** show the quiet region at 800-900 Da. Note that the spectra **B3** contains signals unique for the RBC, demonstrating that peptide/metabolite localization can be facilitated by the system. Enlargement **C1-3** show the peaks of the spiked peptide. This peptide can not penetrate the RBC cell membrane, which is confirmed by its absence in spectra **C3**.

The system for MS analysis of small cell populations demonstrates a potent application of acoustic trapping. Here the controlled microenvironment and viable cell handling offered by acoustic trapping is a major advantage. The simplified approach to acoustic trapping with glass capillaries provides reproducible trapping and aspiration through the open capillary gives a flexible system with low complexity and easy integration to standard equipment.

Cylindrical standing wave resonator for liquid food quality control

Aba Priev

Hebrew University
Dept. of Biochemistry
Jerusalem, 91120
Israel
abbap@ekmd.huji.ac.il

In this review, an innovative technology based on the use of ultrasonic cylindrical standing waves for continuous monitoring of quality of various liquid food products, such as milk, juices, beer, wine and drinking water is described. A proprietary unique feature of the developed ultrasonic analyzer is that it employs a combined mode of operation using both high-intensity and low frequency waves for separation and concentration of the high-molecular-weight particles (fat globules or cells) and low-intensity and high frequency waves for compositional analysis. High accuracy for ultrasound velocity measurements and ultrasound attenuation and rapid testing time (about 30 sec) have been achieved.

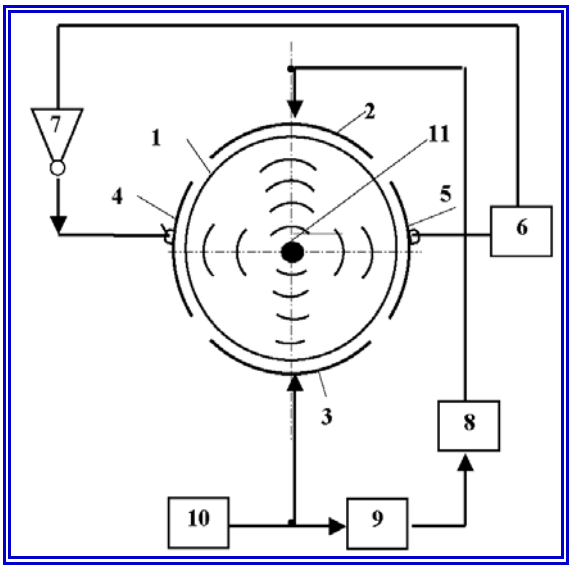

Fig.1. Combines high-intensity unit (10 W/cm^2, 1 MHz) for separation of the particles and low-intensity unit (0.5 W/cm^2, 10 MHz) for compositional analysis after acoustical mixing

Comparative analyses of the ultrasonic method with standard reference techniques have produced linear calibration curves for major components with correlation coefficients higher than 0.95. It is thus possible to monitor total protein and fat content, and somatic cell count in raw milk in cowsheds, or salinity, turbidity, specific gravity, and particles (bacteria) in drinking water directly. Advantages of the proposed technology include the reagent-free nature, no need for sample pre-treatment, ease-of-use, and low cost.

Bubble Motion and Self Organisation in a Microfluidic Channel in the Presence of Ultrasonic Standing Waves

David Rabaud, Philippe Marmottant, Pierre Thibault

Laboratoire SPECTRO
Univ. Joseph Fourier, Grenoble / CNRS
142 Avenue de la Physique
BP87 38402 Saint Martin d'Hères
philippe.marmottant@ujf-grenoble.fr

We report on the primary and secondary acoustic forces exerted by ultrasonic standing waves on the motion of air bubbles in microfluidic devices. Bubbles are generated in a flow-focusing device and various sizes are obtained by adjusting the air to water plus surfactant flow rates. In most situations, bubbles are confined in the height of the channels and their velocity before they enter the acoustic region is controlled by the competition between wall friction and viscous drag due to the liquid flow. Ultrasounds are brought in channel through the resonance modes of a glass rod moulded into PDMS. The plate is placed perpendicular to the downstream channel, and can therefore transmit sound only in localised part of the channel. A CCD camera is used for optical measurements and to record bubble trajectories.

Primary Bjerknes forces cause the very compressible bubbles entering the standing wave region to be deflected and attracted either towards the nodes or the anti-nodes of the standing ultrasonic wave, depending on the relative value of the standing wave frequency and the "squashed" bubbles resonance frequency, as measured on Figure 1. Figure 2 illustrates how this acoustic force of a few hundreds of nanoNewtons in amplitude can be used to drive bubbles in a lab-on-a chip device, by a proper choice of the applied frequency, using moderate sound amplitudes of order of 10kPa.

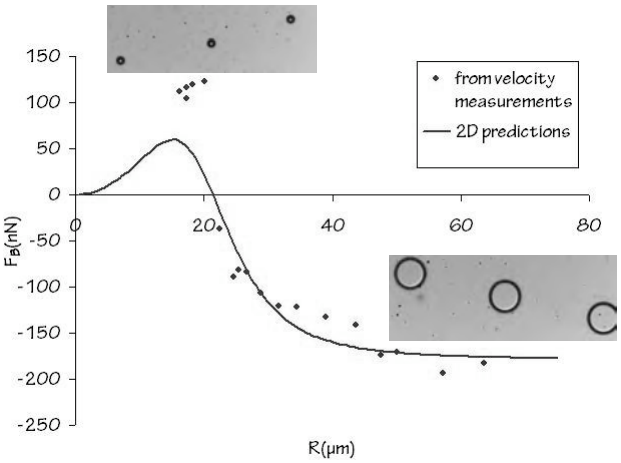

Fig. 1: Measurement of the transverse acoustic force versus bubble radius.

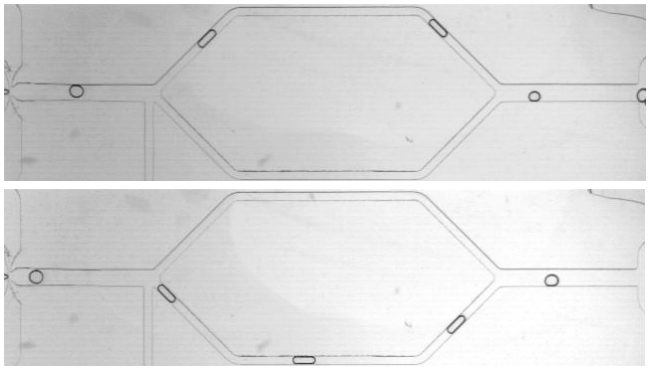

Fig. 2: Top view of a PDMS microfluidic device showing bubbles guided to the upper or lower arm of a channel by changing the acoustic resonance modes. Flow is from left to right. The glass plate resonator, not shown on the figure, is here very large.

Secondary Bjerknes forces between two or more bubbles oscillating in the main pressure field are seen for large pressure amplitudes and/or when the bubbles come close enough. In this case, we observe superimposed to the primary force an additional effect due to the pressure field radiated from one pulsating bubble acting on the second, that makes them either to agglomerate, or to repulse depending on their relative size and of the incident sound. Size sorting experiments using this principle will be presented.

Last, a new phenomenon has been evidenced for moderate incident field amplitudes that manifests by a self-organisation of the bubbles into a periodic lattice, as illustrated by Figure 3. In order to explain the existence of this “bubble crystal” that moves with respects to the acoustic standing wave, existence parameters (size of the bubbles, acoustic amplitude, frequency) have been systematically investigated, leading to a new phenomenological and theoretical description based on bubble-bubble interactions mediated by acoustic waves.

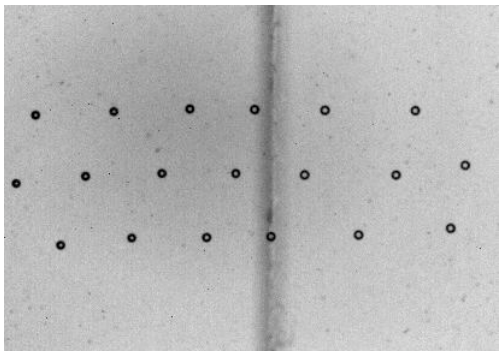

Fig. 3: Self-organization of bubbles (frequency of excitation 87 kHz), the average distance between the bubbles is 335 μm.

Cavitation bubble structures in a standing ultrasonic wave and their cleaning potential

Andrea Otto[1], Till Nowak[1], Robert Mettin[1], Alexander Lippert[2]

and Frank Holsteyns[2]

[1]Georg-August-Universität
Drittes Physikalisches Institut
Friedrich-Hund-Platz 1
37077 Göttingen
Germany
aotto@physik3.gwdg.de

[2]LAM Research AG
SEZ-strasse 1
9500 Villach
Austria
Frankludwig.holsteyns@lamresearch.com

Acoustic cavitation is known to play a key role in many cleaning processes ranging from dental plaque removal to nanoparticle removal from sensitive semiconductor substrates. Unfortunately, the link between process parameters like acoustic field geometry, frequency, intensity or level of gasification and the observed or desired effect is not sufficiently clear. An important aspect of this link is the formation of bubble structures. The applied sound field generates certain bubble distributions in space and time with specific bubble size populations, which in turn mediate the microscopic effects via their oscillation and/or collapse properties.

One aspect of the characterization and comprehension of different bubble structures is the translational behaviour of individual bubbles within a standing ultrasonic wave field[1]. As a result, three groups of bubbles can be distinguished: “large” bubbles, which go to the node; “small” bubbles, which go to the antinode; and “intermediate” bubbles, which have equilibrium positions between the antinode and the node. Moreover, there are translation unstable bubbles, which were named “travelling” bubbles. These latter have no equilibrium space position and have to execute translational reciprocating oscillations between the antinode and the node. Altogether, these individual bubble trajectories lead to a distinct bubble structure. An example is shown in Fig. 1 where ultrasound of 38 or 230 kHz is coupled into a rectangular volume, which is filled with water (transducer positioned at the bottom). ‘Large’ bubbles are visible as bright spots and form horizontal arrays in the nodes. ‘Smaller’ bubbles are observed either in the antinodes for the 38 kHz or seen as streaks travelling throughout the 230 kHz standing wave field.

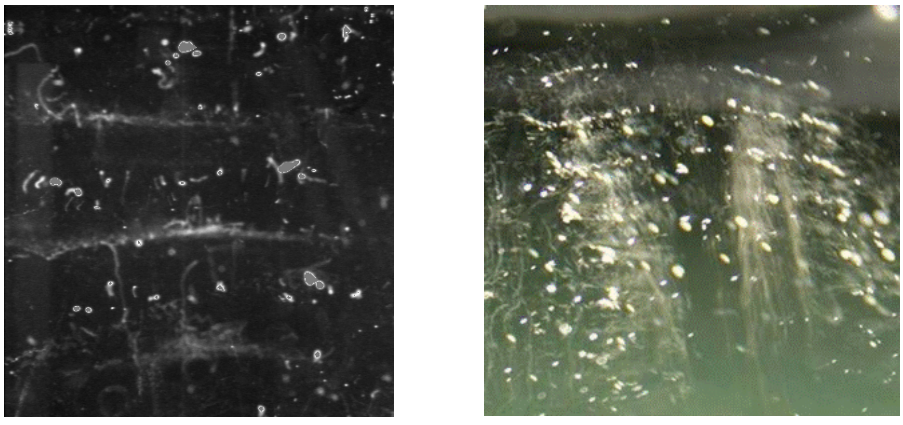

Fig. 1. Photography of the structure from the side in scattered light of a 38 kHz (left) and a 230 kHz (right) acoustic field.

[1] R. Mettin, A. A. Doinikov, "Translational instability of a spherical bubble in a standing ultrasound wave", Applied Acoustics 70 (10), 1330-1339 (2009).

The properties of both types of bubbles were analyzed by direct optical high-speed observations, phase resolved sonoluminescence measurements and their impact on the cleaning of substrates[2]. Thereby it was observed that the bubble arrays in the nodes show striking similarities to the bubble array structures observed by Miller[3] at 1 MHz. An example of such a 'Miller array', which is a line of equidistant and equally sized bubbles, is shown in Fig. 2 for a 40 kHz standing wave field.

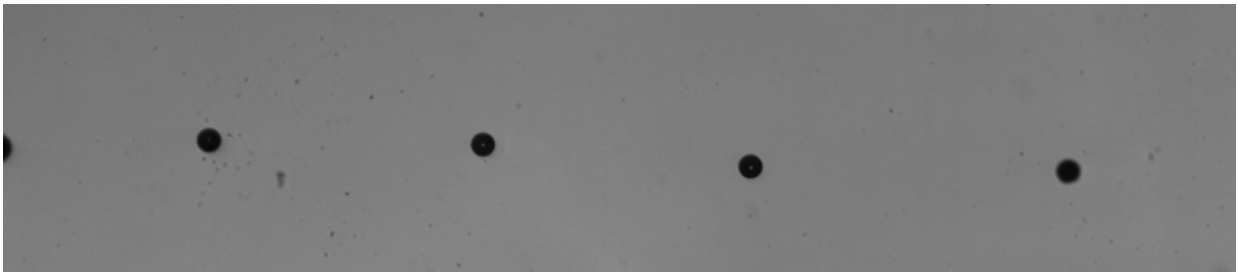

Fig. 2. A Miller array, present in the node of a 40 kHz standing wave field, the bubbles have a characteristic radius of 91 µm.

Under specific conditions, smaller bubbles are accompanying the Miller arrays with fast oscillating translations[4] and eventually become part of the bubble array. At certain positions larger degassing bubbles will appear in the array and disappear due to buoyancy, which leads to the degasification of the liquid. Miller Arrays are observed over a frequency range[5] and typically scale with 1/frequency for parameters such as radius and distance.

The smaller bubbles, running perpendicularly away from the transducer and centrally passing the 'Miller arrays' are the so-called streamers. In the 230 kHz field, which is shown in Fig. 1, the streamers have a typical size between 7-12 µm and velocities of 0.5-1 m/s away from the transducer. A phase resolved sonoluminescence recording[6], as shown in Fig. 3, reveals that the streamers emit light when they pass the pressure anti-nodes. This happens quite synchronously and in relative anti-phase, which reflects the standing wave character of the field.

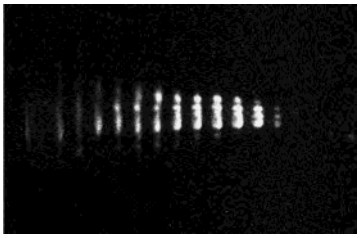

Fig. 3. Sonoluminescence image (time averaged emission). The view is from the side, transducer to the right. The antinodal regions have visible sonoluminescence spots.

Finally, the cleaning potential of both types of bubbles, present in the structure, was tested[2] on the removal of particulate contaminants. We conclude that bubbles, which are part of the Miller array, and the fast streaming bubbles both play a significant role in cleaning processes.

---

[2] A. Otto, T. Nowak, R. Mettin, F. Holsteyns, A. Lippert, "Characterization of a cavitation bubble structure at 230 kHz: bubble population, sonoluminescence, and cleaning potential", in: P. Mertens, M. Meuris, M. Heyns (eds.): Ultra Clean Processing of Semiconductor Surfaces IX, Solid State Phenomena 145-146,Trans Tech Publications, Switzerland, 2009, pp. 11-13.

[3] D. Miller, "Stable arrays of resonant bubbles in a 1-MHz standing-wave acoustic field", J. Acoust. Soc. Am. 62, 12 (1977).

[4] A. Otto, T. Nowak, R. Mettin, F. Holsteyns, A. Lippert, "Investigation of bubble dynamics and sonoluminescence in acoustic fields", Acoustics08, Paris 2008 (oral conference contribution).

[5] A. Otto, T. Nowak, R. Mettin, F. Holsteyns, A. Lippert, "Comparison of cavitation bubble arrays at different frequencies", NAG/DAGA 2009, Rotterdam 2009 (oral conference contribution).

[6] A. Otto, T. Nowak, R. Mettin, F. Holsteyns, A. Lippert, "Untersuchungen zur Kavitation und Reinigung bei Megaschall", in: U. Jekosch, R. Hoffmann (Hrsg.): Fortschritte der Akustik - DAGA 2008 Dresden, Deutsche Gesellschaft für Akustik e.V. (DEGA), Berlin, 2008, pp. 459-460.

"Honey, I shrunk the lab! Acoustically driven microfluidic applications for on-chip laboratories"

Achim Wixforth[1]

[1]Chair for Experimental Physics 1
University of Augsburg
Universitätsstrasse 1
86159 Augsburg
Germany
achim.wixforth@physik.uni-augsburg.de

The term 'microfluidics' comprises the combined efforts of several disciplines to implement small scale fluidic systems for miniaturized hydrodynamic applications. Reduced to small scales, fluids usually behave very different from their macro scale counterparts. It turns out that viscous effects and interactions between the fluid and the (small) vessel walls dominate over inertia effects usually being responsible for the behavior of macroscopic fluidic systems. This dominance leads to a variety of physical differences which - in some cases - are advantageous over macroscopic approaches. In some cases, however, the micro scale laws and effects are not really in favor of a microscale implementation of fluidic devices.

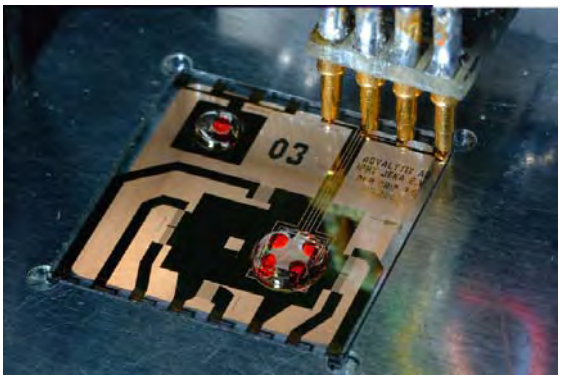

Fig. 1. Fully programmable, acoustically driven lab-on-a-chip for polymerase chain reactions at smallest volumes.

In my talk, I will give an overview over the physical basics of microfluidics, and discuss the pros and cons for actual technological approaches. Many examples will elucidate the special role of physical dimensions in this exciting field.

Then, I present a novel approach to a versatile chip-based microfluidic system with unique properties and functionality. In contrast to many existing microfluidic technologies, the fluid handling is performed on the flat surface of a programmable chip: fluidic tracks and functional blocks such as valves, dispensers, mixers, and sensing elements are chemically defined using standard lithographic techniques. Actuation of the fluid, driving and addressing the functional elements as well as possible sensors are based on electrically excited mechanical acoustic waves, propagating along the surface of a chip. The combination of such fluidic networks and our unique pumping technology results in fully programmable microfluidic processor chips.
Typical areas for the application of this novel technology are the hybridization of DNA or proteomic microarrays, nano-titration stages, on-chip polymerase chain reactions, and cell assays, where single cell manipulation at the planar surface of a chip can be performed. Recent highlights of our research include the observation of a mechanically activated biopolymer being essential for our circulatory system and blood clotting.

Rotation of non spherical particles with amplitude modulation

Thomas Schwarz[1], Guillaume Petit-Pierre[1], Prof. Dr. Jürg Dual[1]

[1]ETH Zurich
Institute of Mechanical Systems
Tannenstrasse 3
8092 Zurich
Switzerland
schwarz@imes.mavt.ethz.ch

Introduction:

The ultrasonic manipulation uses acoustic radiation forces to position particles in predictable locations. In the last years different types of devices have been developed for the manipulation and positioning of micrometer sized spherical particles in lines or more complex patterns [1]. The rotational manipulation of micro-particles in microfluidic devices is another step to expand the possible applications of ultrasonic manipulation. It consists in controlling the angular momentum applied to an object of very small size. The rotation speed as well as the direction of rotation are parameters which must be controlled in order to precisely manipulate the particles. This technique is one of the promising tools which could be used for ultrasonically-driven micro-machines in lab-on-a-chip systems, orientation of fibers in microstructure constructions and positioning of micro-components.

Method:

Non spherical particles behave like spheres in a USW with an additional torque acting on the particle. Fibres shorter than one-fourth of the wavelength are constrained at the pressure node and are oriented perpendicular to that of wave propagation [2]. It is possible to use this acoustic radiation torque for a continuous and controlled rotation of objects. Therefore a time-varying pressure field with change of orientation of the potential well is needed.

Oberti *et al.* [1] studied the different cases of the superposition of two orthogonal standing waves generating a two-dimensional pressure field. These results are of great interest in this special case, they represent a starting point for the rotation of particles.

The method is extended here to the amplitude modulation of two orthogonal standing waves. By varying the amplitudes of the standing waves the orientation of the force potential minima, indicated by the black arrow in figure 1, could be rotated.

Figure 1 shows the force potential for the amplitude decrease of the standing wave in x direction, from +1 to -1, while the amplitude in z-direction is set to a constant value. Figure 2 shows the inverse case, with decrease of the amplitude in z-direction, while the amplitude in x-direction is set to a constant value. The combination of the force potentials of figure 1 and 2 leads to a rotation of 180°.

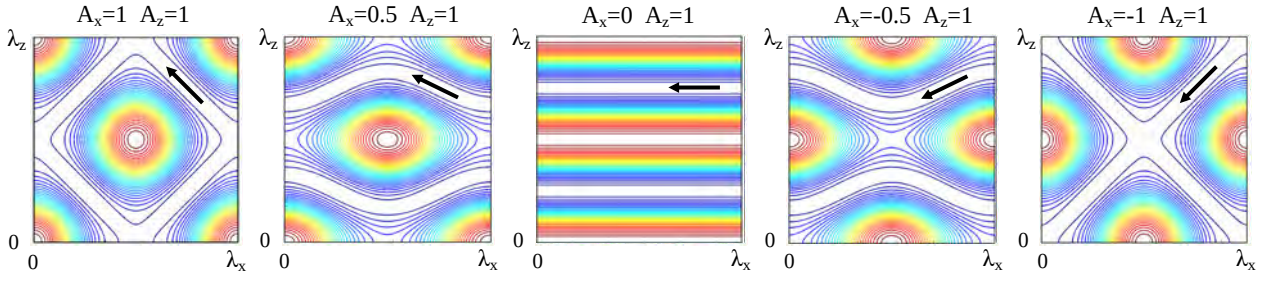

Fig. 1: Contour plot sequence of the Gor'kov force potential as result of amplitude change in x-direction resulting from superposition of two in phase cosine functions with identical frequency. The term A_x varies from +1 to -1. The red areas are potential maxima, the blue areas potential minima. The black arrow is representing a fiber at the force potential minima.

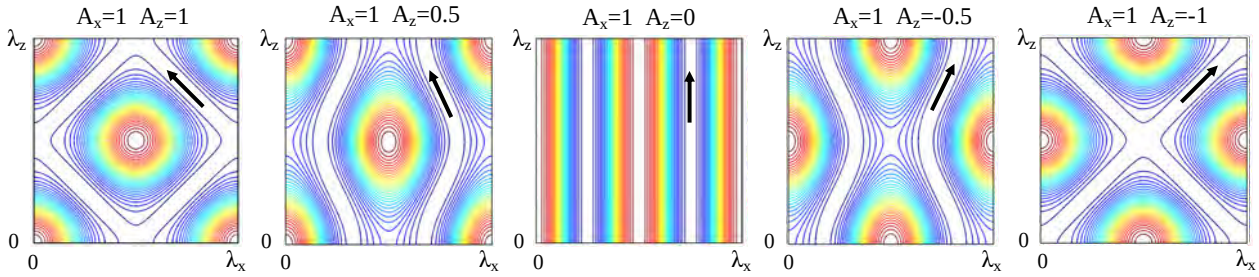

Fig. 2: Contour plot sequence of the Gor'kov force potential as result of amplitude change in z-direction resulting from superposition of two in phase cosine functions with identical frequency. The term A_z varies from +1 to -1. The red areas are potential maxima, the blue areas potential minima. The black arrow is representing a fiber at the force potential minima.

Results:

The device used for the experiments consists of a 3x3 mm^2 chamber etched into Silicon and covered with a glass plate. The actuation is done through a 4x4 mm^2 piezoelectric crystal fixed at the back side of the device. By exciting two orthogonally oriented strip electrodes, defined on the surface of the same piezoelectric transducer, a two dimensional pressure field can be set up, assuming that the chamber depth is kept smaller than half of the acoustic wavelength in the fluid [1].

Figure 3 shows the complete rotation of a 200 µm long glass fiber. The actuation frequency was set to 1085 kHz with a maximum amplitude of 30 V. The speed of rotation could be increased until about 30 rpm. Additionally, it was possible to stop the fiber at any given orientation and it was possible to inverse the rotational direction.

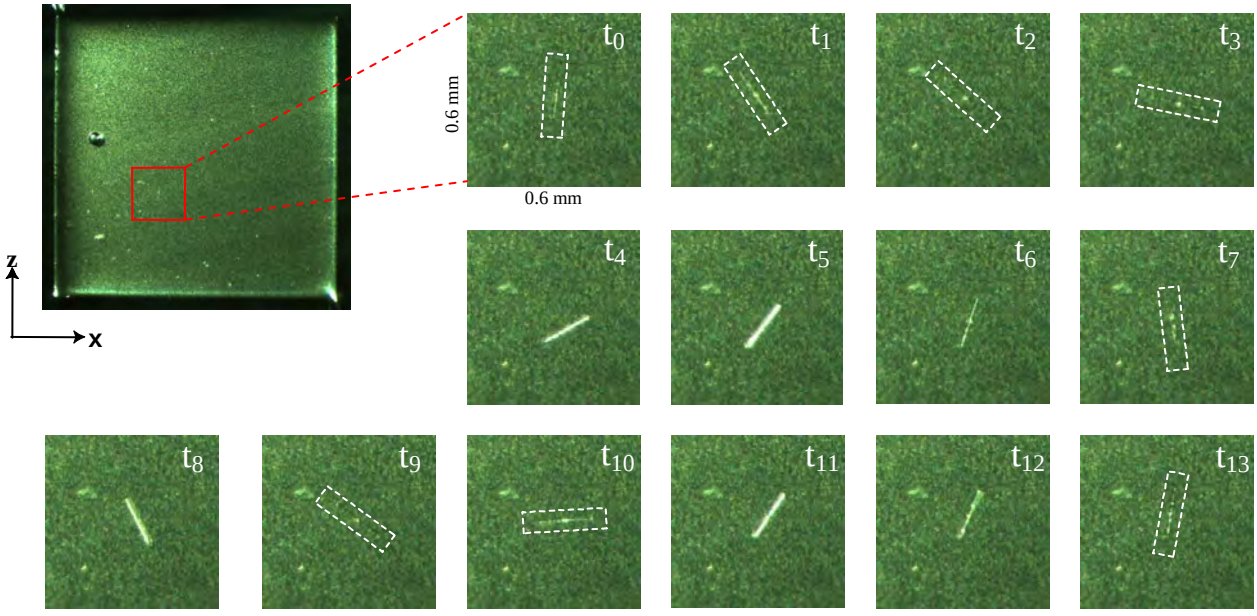

Fig. 3: A 360° rotation of a 200 µm length fiber due to the amplitude modulation of two orthogonal standing waves. The sequence is imported of a video and shows a 0.6x0.6 mm^2 zone; the images are spaced of 0.12 s. The frequency actuation is f = 1085 kHz for both standing waves. The dashed white rectangle helps to visualize the fiber.

[1] Oberti, Neild, Dual, J. Acoust. Soc. Am., 121 (2007), pp.778-785
[2] Yamahira, Hatanaka, Kuwabara, Asai, Jpn. J. Appl.Phys. Vol.39 (2000) pp.3683-3687

Control of the unidirectional particle motion in the channel of vibrating multilayer plastic microdevices

Itzíar González[1], Tomás Gómez[1]

[1]Spanish National Research Council CSIC
Institute of Acoustics
Dept. of Ultrasounds
Serrano144
2006 Madrid
Spain
iacgg38@ia.cetef.csic.es

A plastic microdevice is presented in this work to carry out ultrasonic micromanipulation of particles within a channel slightly wider than a quarter of wavelength along which suspensions flow. It is an asymmetrical device built in a soft material, SU-8, already presented in USWNET-Zurich-2008[1] with a microfluidic channel and a piezoelectric ceramic attached to one of its outer edges. Use of SU8 instead of silicon may present the drawback of having much weaker channel resonances but presents some other advantages. This device (Fig. 1) behaves as a multilayer system in which all the layers (including a not resonating channel) are involved in the establishment of a standing wave across their width. That part of the wave established within the channel includes a node or antinode of pressure (depending on the requirements of the sample for the particle manipulation), strategically located, toward where the flowing particles are driven by a radiation force acoustically induced, perpendicular to the flow direction

Fig. 1. Ultrasonic microdevice for particle micromanipulation

The width of the channel is somewhat larger than a quarter of a wavelength, which does not fit any of the conventional models but it represents an intermediate situation. A strategic combination of the width of the different layers conforming the chip allows the establishment of a node or antinode of pressure inside the channel at the desired location, depending of the requirements of every specific application (either sorting/separation or agglomeration processes). In the case of suspensions containing particles with positive acoustic contrast factors ($\Phi>0$) a node of pressure is required inside the channel to collect the microelements, for which determined specifications of the chip configuration are demanded. On the contrary, in the case of samples with negative values of Φ, an antinode of pressure must be generated inside the channel at the same desired location instead of the node to collect the particles driven by the axial radiation force. This is relatively easy to achieve in a multilayer system modifying some parameters, like the width of the plastic layers of the chip surrounding the channel of treatment.

Numerical modelling of the multilayer system

A multilayered 1D model based on a general formulation of the matrix transfer function that includes the piezoelectric effect in the actuator, the electric loads and the exact material parameters is proposed to model the response of the chip and the actual acoustic field distribution within the channel.

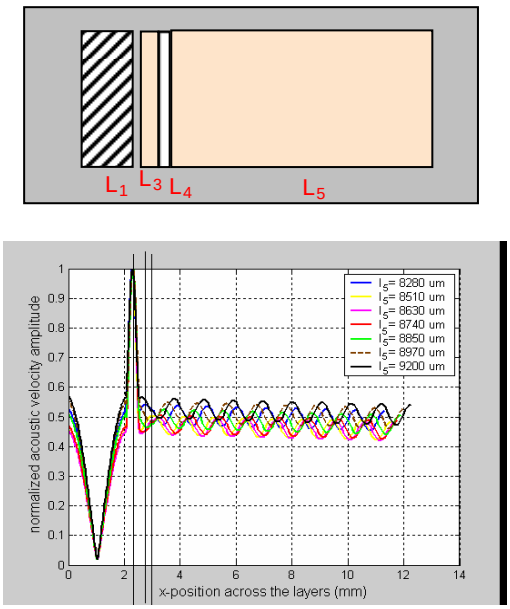

Figure 2: numerical simulation (Matlab) of the standing wave establishment across the different layers width of the device

Apparent displacements of the pressure node are numerically expected for small variations of the channel location within the chip, slightly larger than λ/8.

Experimental analysis of the particle motion within the channel

Diverse sets of experiments have been carried out with aqueous suspensions of polystyrene particles, for which two different chip configurations have been performed with different plastic layer widths surrounding the channel. Appreciable displacements of the node of pressure collecting the particles were observed when the distance between the channel and the piezoelectric actuator was increased something less than a quarter of wavelength, about λ/6. (Fig. 3)

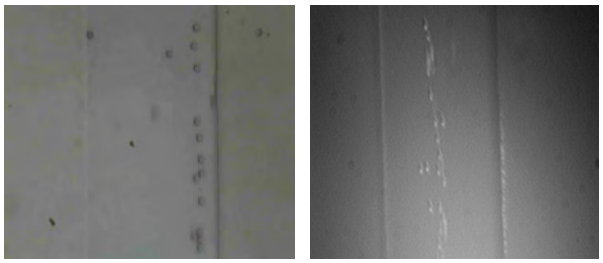

l_3=750µm l_3=500µm

Figure 3: particle collection along the node of pressure inside the channel at f=880 kHz,

Both, theoretical and experimental results show similar displacements of the node of pressure within the channel for different chip configurations differentiated by variations of the distance between the channel and the piezoelectric ceramic smaller than λ/6 working at a same frequency.

[1] http://www.uswnet.org/docs/USWNet2008_book_of_abstracts.pdf

Reducing particle size dispersion in free flow acoustophoresis using 2D acoustic prefocusing

Carl Grenvall, Per Augustsson and Thomas Laurell

Lund University
Dept. of Electrical Measuremensts
E-building, LTH
Ole Römers väg 3
223 63 Lund
Sweden
carl.grenvall@elmat.lth.se

This paper presents a 2-dimensional acoustic standing wave mode of operation in free flow acoustophoresis (FFA). A vastly improved size dispersion profile is obtained as compared to previous work by prefocusing the particle sample stream into a confined well defined flow stream with uniform velocity, using a 2-dimensional standing wave pattern, prior to entering the FFA separation zone.

Introduction

Strategies for particle and cell separations in microfluidic systems are highly desired. In view of this FFA has emerged as an attractive tool since the separation is based on the intrinsic acoustic properties of particles or cells. Petersson et al. [1] demonstrated continuous FFA size separation of particles mixtures in the range of 2-10 µm as well as blood component fractionation. In FFA the particle stream is laminated along the side wall of a flow channel that supports a λ/2 standing wave. The particles migrate to the standing wave pressure node in the channel center, and as the migration speed scales with the square of the particle size a lateral distribution of particles across the channel width is obtained, Fig 1. A key limiting factor in the original FFA separation system was the initial spatial distribution of particles at the inlet in combination with the inherent parabolic flow profile of the microchannel. This resulted in varying duration times in the acoustic force field and, thus, the lateral displacement of a given particle size displayed a "peak broadening". In order to overcome this we have now included a 2-dimensional prefocusing step of the particle stream prior to entering the acoustic separation zone, which confines the particles to a distinct position of the flow stream yielding uniform flow velocities. 2-dimensional continuous flow focusing has previously proven successful in acoustically activated cell sorting work [2].

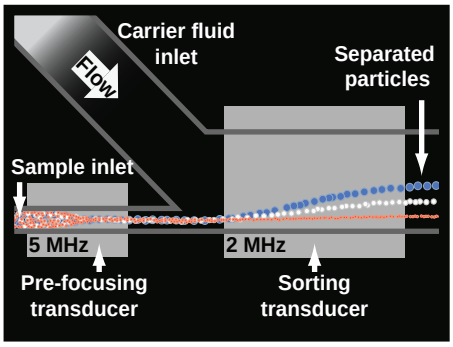

Fig. 1. FFA principle. Pre focused particles are laminated near the FFA channel side wall and migrates to an acoustic standing wave node in the channel center at a velocity based on their size

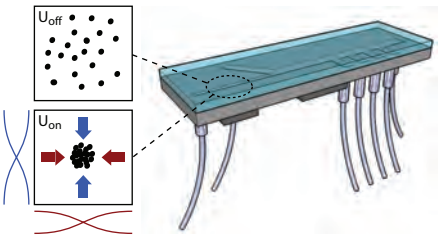

Fig. 2. The FFA device includes a 2-dimensional pre focusing step which focuses particles to the center of the sample inlet channel. (Left) The square channel crossection with particles before and after pre focusing.

Experimental

Fig 2 shows a schematic of the new FFA design. The prefocusing zone is designed as a square cross-section (inserts) flow channel (150 µm by 150 µm), which allows particles to be simultaneously focused laterally and vertically using a 4.88 MHz transducer. The prefocused particle stream is hydrodynamically laminated to the side wall of the main channel (375 µm wide, actuated by a second transducer at 1.91 MHz) so as to utilize the full half width of the separation channel for the separation process. As model system we prepared a ~1.4% by volume polystyrene particle mixture of 3 µm (0.15% by volume), 7 µm (0.65% by volume) and 10 µm (0.60% by volume).

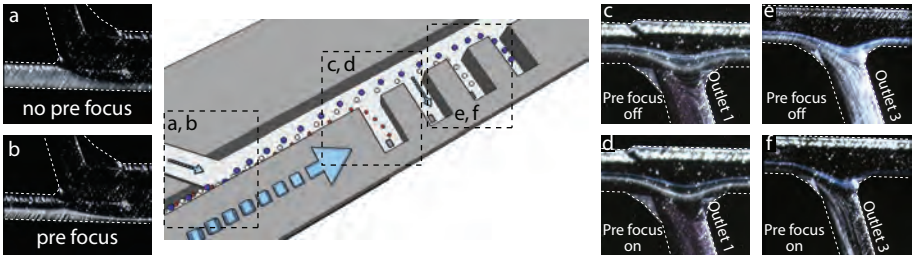

Fig. 3. Particles enter the channel through a pre focusing (b). After prefocusing the particles are hydrodynamically laminated along the channel wall and then separated using FFA. Insert pictures show particle dispersion during the experiment with prefocusing inactive (top inserts) and activated.

Results and discussion

Ocular inspection from different angles revealed particles to be focused laterally as well as vertically. Fig 3 shows the prefocusing channel with the prefocusing actuator active/inactive. Analysis by particle counting revealed a significantly improved sorting capability when using prefocused particles compared to non focused particles. Inactive prefocusing recovered ~95%, ~74% and ~84% of the 3, 7 and 10 µm particles into the intended outlet, Fig 4. Activation of the prefocusing channel increased the separation efficiencies to ~97%, ~93% and ~99% for the 3, 7 and 10 µm particles, respectively, Fig 5.

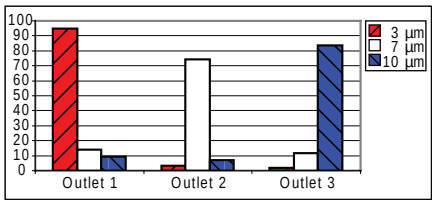

Fig. 4. Histogram showing the relative distribution of each particle size in the three outlets with 2D-prefocusing inactive.

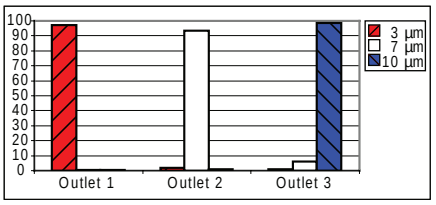

Fig. 5. Histogram showing the relative distribution of each particle size in the three outlets with 2D-prefocusing activated.

Conclusions

The presented FFA chip constitutes a significant improvement compared to previous work. For the first time a 2-dimensional acoustic prefocusing segment has been implemented in a particle separation system based on intrinsic acoustic properties. The reduced particle dispersion opens up for significantly increased separation resolution for cell separation purposes in future work.

Acknowledgements

Vinnova programme Multidisciplinary Bio, Swedish Research Council, Royal Physiographic Society in Lund, Crafoord Foundation, and Carl Trygger Foundation are acknowledged for their support.

References

[1] F. Petersson, L. Åberg, A-M. Swärd-Nilsson and T Laurell, Anal Chem 79 (14) 5117-23, (2007)

[2] C. Grenvall, P. Augustsson, F. Petersson and T. Laurell, Fluorescent activated cell sorter using ultrasound standing waves in microchannels, Micro Total Analysis Systems 2007, Paris, France (2007)

Modelling of a standing surface acoustic wave device for flow cytometry in an oceanographic sensor

Michael J. Gedge, Rosemary J. Boltryk, Peter Glynne-Jones, Martyn Hill.

University of Southampton
School of Engineering Sciences
Southampton
United Kingdom
m.gedge@soton.ac.uk

Background, Motivation and Objectives

The Earth's oceans host an enormous range of natural resources. They are a crucial element of our transport and energy infrastructures, and they play an overriding role in climate regulation. Monitoring the biological and chemical characteristics of the oceans is essential in the generation and verification of reliable models of the global ecosystem.

Existing methods for carrying out such monitoring typically rely on the acquisition of water samples for subsequent laboratory analysis. This approach is expensive, is inevitably coarse in terms of spatial and temporal sampling, and involves significant risk of sample contamination and degradation. Continuous and distributed monitoring of the oceanic environment requires biochemical sensor platforms that are small, robust, reliable, and power efficient. Ultrasonic technologies have the potential to offer a low power route to address a number of issues in a remote marine measurement system, including barrier-free pre-filtration, sample concentration, and sample focussing.

Designing a sensor that uses acoustic radiation forces for use in oceanographic environments poses many challenges, not least because variations in salinity and temperature significantly affect the acoustic behaviour. The harsh environments and high pressures play a part in material selection and acoustic design.

Shi *et al.* (Lab on a Chip 2008) demonstrated the focussing of particles in two dimensions using standing surface acoustic waves. This was achieved using a Lithium Niobate transducer and a PDMS fluid channel. This has the potential to be used in a flow cytometry device for oceanographic sensing of biological matter. A significant advantage of using acoustic based focusing is that there is no need for sheath flows and hence a reduction in the volume of reagents that need to be carried by the remote sensor. The aim of this research is to improve the understanding of the mechanisms involved, to investigate the robustness of such a device, and to optimise it for use in the challenging oceanographic environment. We discuss the results from finite element analysis simulation used to investigate resulting acoustic forces which focus particulates and the fabrication of the sensor chip.

Discussion

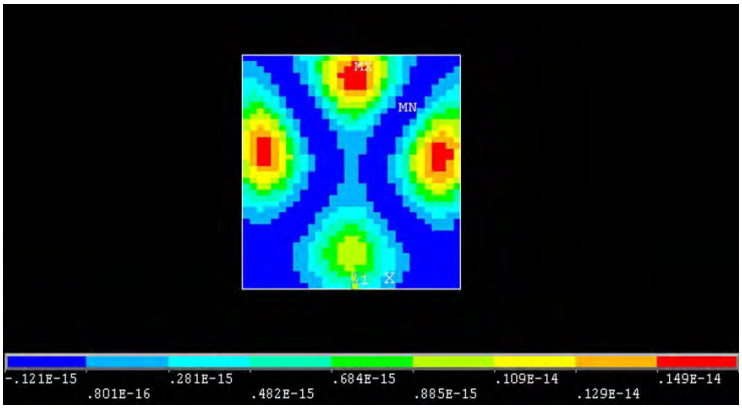

Fig. 1 Acoustic radiation force potential showing mode with significant coupling from PDMS walls.

The paper presents a computational study into the mechanisms involved and the effects of dimensions and materials on the behaviour of a surface standing acoustic wave device. The modelling suggests the existence of modes that will cause particles to align in the centre of a square channel, but also suggests other modes with very strong coupling between the highly complaint walls and the fluid channel (see Fig. 1). The predicted forces are of the order of tens of pN. The modelling has also been used to investigate the sensitivity of the modes to manufacturing tolerances and material properties. A prototype (shown in has been designed and fabricated and is currently being tested

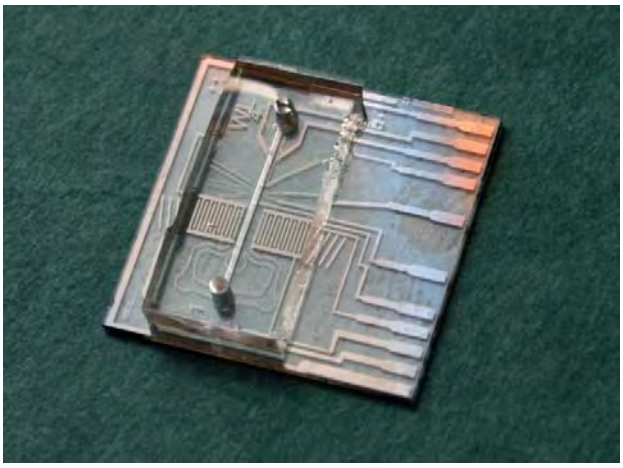

Fig. 2. Prototype device.

Modelling has demonstrated the suitability of a standing surface acoustic wave device for use in a flow cytometry oceanographic sensor. The validity of these results is currently being tested with a series of prototypes. The predicted mode is strong; however, it is sensitive to various design parameters.

Flow-free transport of particles in a macro scale chamber

Dirk Möller[1], Jurg Dual[1]

[1]Institute of Mechanical Systems
Dept. of Mechanical and Process Eng.
ETH Zurich
CH-8092 Zurich
Switzerland
dirk.moeller@imes.mavt.ethz.ch

Introduction

The use of acoustic forces has been shown to be a promising solution for systems where mechanical contact is a drawback. There are many reports on flow-through systems which are operated at a single frequency, such that the suspended particles are concentrated into parallel planes in one dimensional standing pressure fields[1]. On the other hand there are needs for concentration of particles in batch mode, such as achieved with sedimentation or centrifugation. These methods also allow operation in a sealed compartment, but are limited by either Brownian motion or lead to tightly packed agglomerates. Another solution is therefore the use of acoustics.

Method

Flow-free transport of a large number of particles in a batch mode system can be achieved by setting up a beat frequency with two slightly different excitation frequencies at opposite ends of a square chamber or by a fast frequency ramping. Particles can also be transported by setting up a standing pressure field at different frequencies, either with frequency hopping or sweeping[2, 3, 4]. Here the later is discussed with an asymmetric excitation, such that an overall movement in one direction at all places within the device can be realised. The boundary which is set to vibration acts as a variable boundary. Therefore by increasing the frequency and with it the number of nodal planes, particles can be moved away from the excitation or, by decreasing the frequency continuously, particles can be moved towards the excitation boundary.

Results

Repeated frequency sweeping in a range from 1.5MHz to 2.5MHz has been used in a square (23 x 23 x 5mm) plastic (PE) chamber to collect particles along one of the sidewalls. Operating with particles with a diameter of 9µm, about 80% to 90% of the particles can be concentrated within less than 2min. Time and yield are significantly increased with 26µm particles.

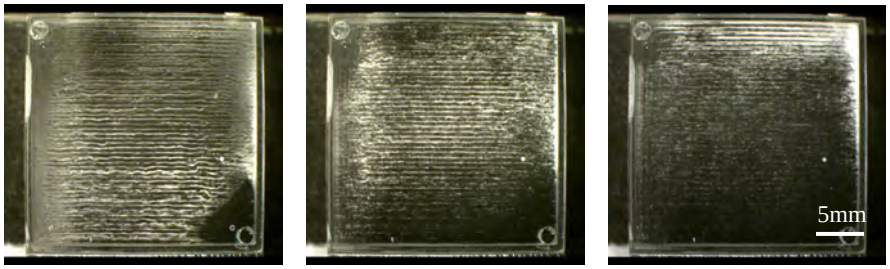

Fig. 1. Concentration of 9µm particles with a repeated frequency sweep (1.5MHz – 2.5MHz). The particle distribution is shown in initial condition on the left image, after 40s in the second image and after 120s in the third image.

[1] T. Laurell, F Petersson and A Nilsson, Chem. Soc. Rev., 36 (2007), pp. 492-506
[2] M. Saito, N. Kitamura and M. Terauchi, Jour. Of Appl. Physics, vol 92, no 12, 12 (2002), pp. 7581-7586
[3] A. Haake, Micromanipulation of Small Particles with Ultrasound, Diss. ETH No. 15681
[4] G. Whiteworth, M.A. Grundy and W.T. Coakley, Ultrasonics, vol 29 ,12 (1991), pp. 439-444

Characterization of acoustic streaming in an ultrasonic cage

Mathias Ohlin, Otto Manneberg and Martin Wiklund

Royal Institute of Technology
Dept. of Applied Physics
KTH - Albanova
SE-106 91 Stockholm
Sweden
martin@biox.kth.se

Introduction

We have previously described a microfluidic chip designed for 3D ultrasonic caging of individual cells (see Fig. 1) [1, 2]. One cage is a 300×300×110 μm^3 square-shaped chamber integrated in a 300×110 μm^2 cross-section flow channel (see Fig. 2). The other cage has a round confocal design with a diameter of 300 µm and the same flow channel dimensions as for the square-shaped chamber (see Fig. 3). In the present abstract, we use micro Particle Image Velocimetry (µPIV) for investigating the acoustic streaming induced in the cages when operated around 2.5 and 6.9 MHz.

Procedure and method

The chip was operated according to the procedure described in Ref. 1. A further development of the already existing µPIV toolbox for Matlab [3,4] was performed in order to quantify the speed and direction of the acoustic streaming. The developed Matlab program (see Fig. 4) plots vector fields to represent the velocity distribution of tracer particles (1-µm beads). Using a camera (Zeiss AxioCam HSc) and a microscope (Zeiss Axiovert 135) images were acquired of the different chambers in the microfluidic chips (see Fig. 1). µPIV was then performed on pairs of consecutive images or on sets of several images. Cross-correlation was the main method of choice when performing µPIV using an interrogation window size of 32x32 pixels and an overlap of 70 %. In both the square-shaped chamber as well as in the round confocal chamber the streaming showed a constant motion over several images. This made it possible to average over several images and calculate the truncated mean value discarding the zero valued vectors. The result from the µPIV simulations of both the square-shaped and the round confocal chamber can be seen in Figs. 5 and 6. From the plots it is clear that the induced Rayleigh-type streaming has a maximum speed in the order of 100-200 µm/s for the actuation voltage 10 V_{pp}.

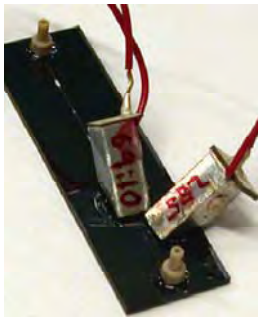

Fig. 1. Microfluidic chip with two mounted wedge transducers. 2.5 MHz for focusing and 6.9 MHz for levitation.

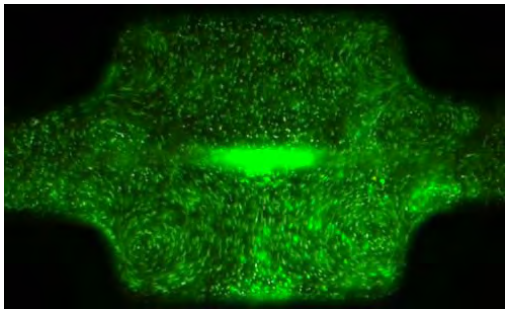

Fig. 2. Round confocal chamber

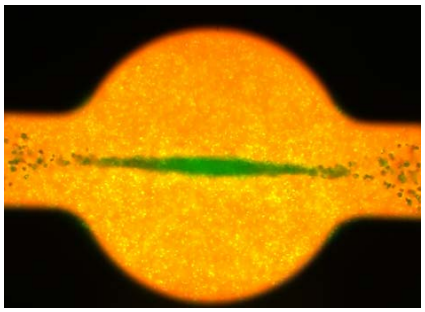

Fig. 3. Square-shaped chamber

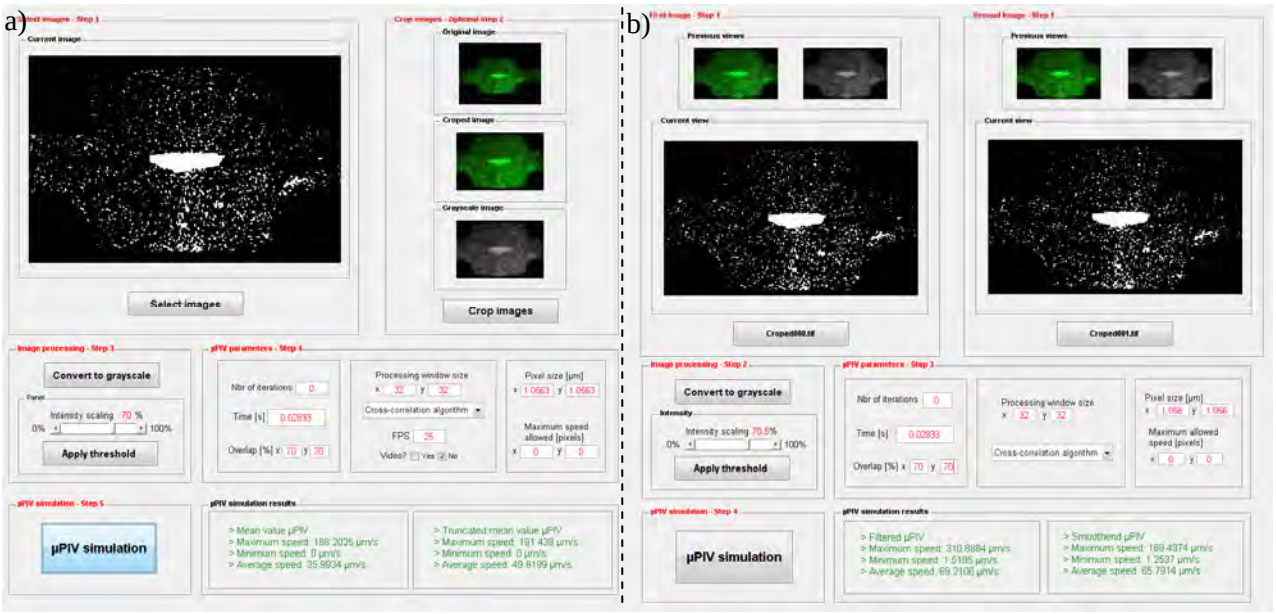

Fig. 4 The developed Matlab program. These are the two graphical user interfaces for µPIV simulations on sets (a) and pairs (b) of consecutive images.

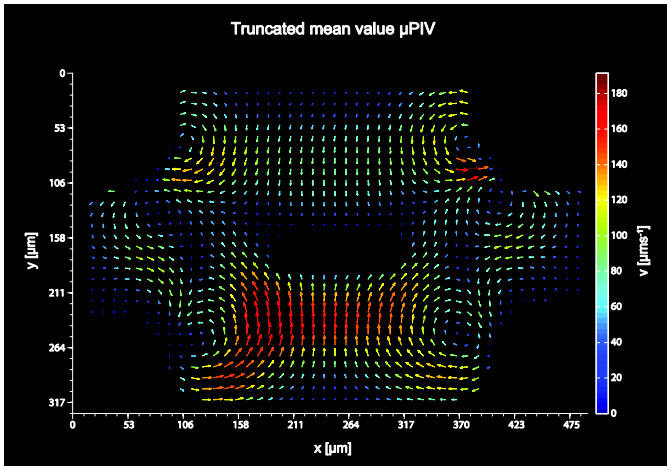

Fig. 5 Plot generated from µPIV simulation data using the square-shaped chamber (cf. Fig. 2).

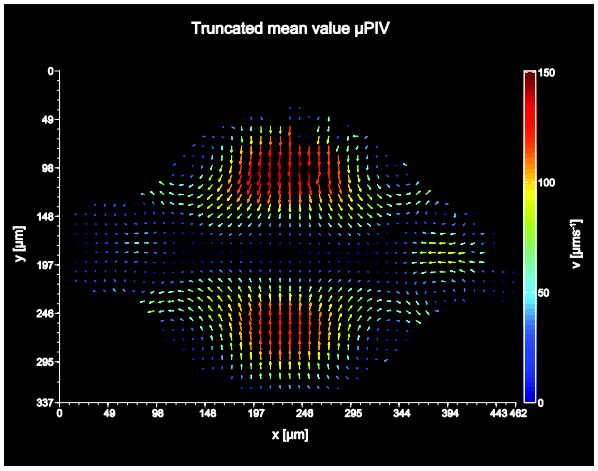

Fig. 6 Plot generated from µPIV simulation data using the round confocal chamber (cf. Fig. 3).

Result and discussion

From the diagrams we see that the square-shaped cage has a more asymmetric and complex pattern of the streaming vortices, including vortices with both horizontal and vertical rotation axes. On the other hand, the pattern in the round cage is more symmetric with dominating vortices having horizontal rotation axes.

References:

[1] O. Manneberg, B. Vanherberghen, J. Svennebring, H. M. Hertz, B. Önfelt and M. Wiklund, *"A three-dimensional ultrasonic cage for characterization of individual cells"*, Appl. Phys. Lett. **93**, 063901 (2008).

[2] O. Manneberg, B. Vanherberghen, B. Önfelt and M. Wiklund, *"Flow-free transport of cells in microchannels by frequency-modulated ultrasound"*, Lab Chip **9**, 833-837 (2009).

[3] MPIV toolbox for Matlab, http://www.oceanwave.jp/softwares/mpiv/.

[4] http://www2.imm.dtu.dk/~hbn/dace/.

An ultrasonic particle trap using 3-D structures

A. Hughes, J. Hill, R. Jones, T. Purchase, M. Hill, R. J. Boltryk, M. Gedge, P. Glynne-Jones

School of Engineering Sciences
University of Southampton
Southampton
SO17 1BJ
UK
R.J.Boltryk@soton.ac.uk

Introduction

We describe the development of a device designed to collect a concentrate of cells for environmental monitoring and bio-hazard detection using ultrasonic radiation forces. To avoid problems associated with continuous separation of a concentrated stream of particles, a batch trapping procedure is used where trapped cells are periodically eluted from the trapping site through a high concentration outlet.

Design and construction

To generate trapping forces which oppose the flow a series of machined pegs are used to generate a complex 3-dimensional field and therefore radiations forces acting axially, laterally and against the flow direction. Finite element analysis (ANSYS) was used to investigate the acoustic field around the pegs with the final design machined into macor, a glass ceramic. Fig. 1 depicts the trapping chamber which is encapsulated by a glass reflector layer.

Results

Experiments show that both 20 and 1µm diameter polystyrene beads can be trapped against a flow over a period while clarified flow is passed through and removed from the system (Fig. 2). Both finite element and experimental results suggest that the pegs give rise to lateral trapping forces generated by a combination of enclosure and structural modes, especially of the pegs themselves. On reaching a saturation level where no additional beads become trapped, these beads can then be eluted by switching off the ultrasonic field and increasing the flow rate. In this way a 10 times increase in concentration was collected for 20 µm beads. Future work will look at eluting the beads through a separate outlet to avoid dilution of the processed sample with clarified flow.

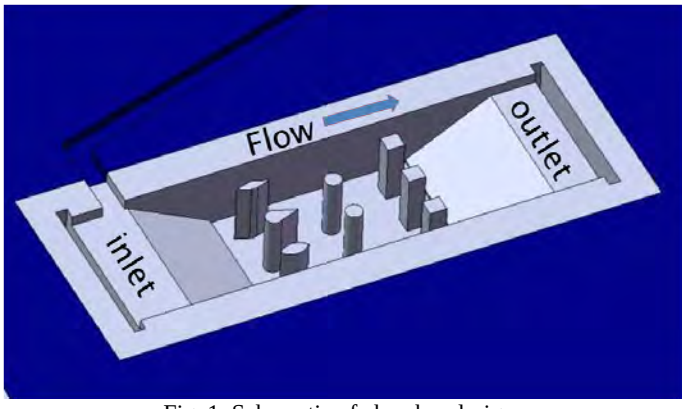

Fig. 1. Schematic of chamber design.

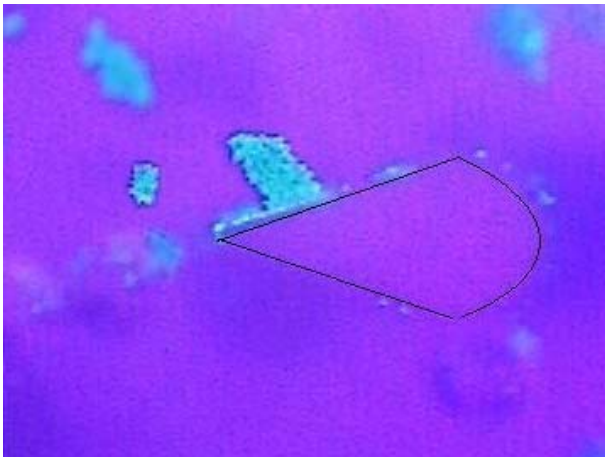

Fig. 2. Agglomeration of particles around peg.

Acoustic evaluation of ion-exchange dynamics using a single resin bead

Takahiro Kanazaki[1], Tetsuo Okada[1]

[1]Department of Chemistry
Tokyo Institute of Technology,
Meguro-ku, Tokyo 152-8551, Japan
tokada@chem.titech.ac.jp

There remains no room for scientific or technological innovation in ion-exchange, because it is a matured technique and established theories well describe relevant equilibria. Is it true? Thermodynamics involved therein has actually been well elucidated by conventional work in this discipline. In contrast, the molecular processes of ion-exchange have not been understood very well. This unbalanced advancement in ion-exchange fundamentals comes from the lack of appropriate methods for studying the molecular process of ion-exchange. Conventional methods for ion-exchange studies strongly rely on chemical analyses, which require a relatively long time period for measurements as well as a bulk amount of ion-exchange materials. The development of *in situ* measurements with a single ion-exchange bead is thus expected to reveal the dynamics of ion-exchange process and to lead to the further developments of chemistry of ion-exchange.

Methods

A single cation-exchange bead fully loaded by a particular countercation was entrapped in an ultrasonic standing wave (500 kHz) in an aqueous solution containing of an external cation. The acoustic radiation force was balanced with a sedimentation force by the vertical generation of the ultrasound. A resin bead was levitated slightly below the node of the standing wave according to its acoustic properties and the intensity of an ultrasonic radiation force. The introduction of a single bead of Dowex 50W X-8 into a cell allowed the initiation of the ion-exchange reaction between internal and external cations. The levitation coordinates were read out from the pictures taken every ca 5 sec.

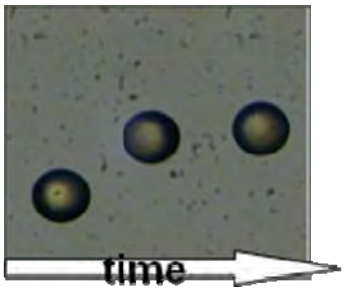

Fig.1 Time-change in levitation coordinate with the progress of ion-exchange reaction

Results and Discussion

The levitation coordinate depends on the acoustic properties of an ion-exchange resin bead, which are determined by its density and compressibility. These properties basically come from the nature of a countercation, and thus the levitation coordinate is changed as the ion-exchange reaction between the initial countercation and an external cation proceeds. Fig.1 shows a time-change in the levitation coordinate of an ion-exchange resin bead with the progress of ion-exchange between internal K^+ and external H^+. The K^+-form resin is less buoyant than the H^+-form counterpart because the former is denser than the latter; though the latter has lower compressibility, the density dominates the resin bead behaviour in this particular case. The levitation position of the resin bead therefore becomes higher as H^+ invades the bead and replaces K^+ in it. The exchange ratios calculated from levitation coordinates were plotted against the time elapsed from the initiation of the reaction for resin beads with different

sizes in Fig.2. The plots imply that the reaction is completed within 100-150 sec for the resin beads with the diameters of 66-127 μm. The results shown in this figure were analyzed on the basis of the Nernst-Planck equation.

$$J_A = -D_A[\mathrm{grad}C_A + z_A C_A (F/RT)\mathrm{grad}\varphi]$$

$$J_B = -D_B[\mathrm{grad}C_B + z_B C_B (F/RT)\mathrm{grad}\varphi]$$

$$z_A C_A + z_B C_B = C = \mathrm{const}$$

$$z_A J_A + z_B J_B = 0$$

where A and B denote an ion initially present in a bead and that in an external solution, respectively. The last two equations indicate electrical neutrality and no electric current, respectively. The results of numerical analyses obtained for a 80 μm (solid curve) and a 120 μm (dotted curve) resin bead are also depicted in this figure. The literature diffusion coefficient for H^+ in the same resin (D_H=6.38×10^{-10} m^{2}sec^{-1}) was used for these calculations, which gave D_K =ca 3×10^{-11} m^{2}sec^{-1}. This diffusion coefficient for K^+ agrees well with the reported value determined with a radio isotope. Ion-exchange reactions for different cations can be studied in a similar fashion. In the presentation, ion-exchange between H^+ and Cs^+ or tetraethylammonium ion is also discussed.

Hence, the proposed method is efficient for the dynamic evaluation of ion-exchange processes with a single resin bead. The resin beads are not necessarily identical and may have different physical/chemical properties. Such aspects cannot be evaluated by the conventional methods, in which a number of resin particles should be used for experiments; the average properties are thereby revealed. The acoustic method can thus be utilized to evaluate the individuality of resin beads as well.

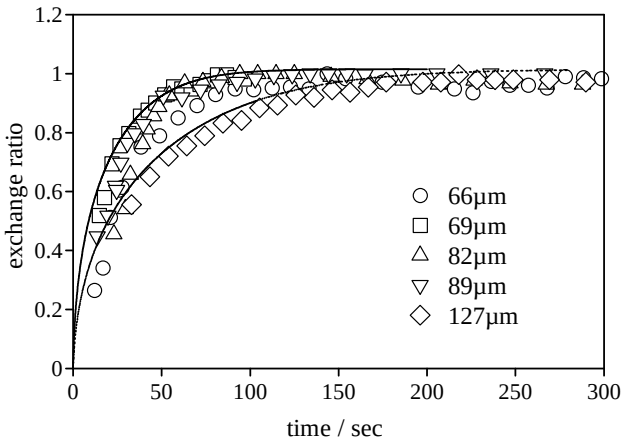

Fig. 2 Time changes in ion-exchange ratios
K^+ in a resin bead was replaced by H^+ in an external solution (0.05 M sulphuric acid). Solid and dotted curves show the results of calculation based on the Nernst-Planck equation. The diffusion coefficient for H^+ in Dowex 50W X-8 resin (6.38×10^{-10} m^{2}sec^{-1}) was taken from literature, and that for K^+ was assumed to be 3×10^{-11} m^{2}sec^{-1}.

Characterising a particle trap for the monitoring of ion-exchange processes

Rosie Boltryk[1], S. Hirawa[2], T. Okada[2], P. Glynne-Jones[1], M. Hill[1]

[1] School of Engineering Sciences
University of Southampton
Southampton, UK
R.J.Boltryk@soton.ac.uk

[2] Department of Chemistry
Tokyo Institute of Technology
Tokyo, Japan

Overview

The trapping of particles or cells using ultrasonic radiation forces is relevant to a range of biological, chemical and medical analyses, for example, those involving cell washing, cell separation or testing of reagents. This work studies the trapping forces within a flow-through chamber designed to detect counterions based on the aggregation position of ion-exchange resin beads. Certain counterions alter the water content of the beads and therefore their acoustic properties; this in turn alters the acoustic contrast factor, and thus the magnitude of the acoustic radiation force acting upon them. This causes the equilibrium position of the beads to alter when the radiation force is acting against either gravity or fluid drag forces.

Method

We consider a device (Fig. 1) used to trap a bead within a resonant channel and against fluid flow. The spatial variation of the acoustic radiation force along the length of a resonant channel is of interest here and a finite element model (ANSYS) is used to predict the acoustic field and the radiation force potential. This data is processed in MATLAB to predict where particles will agglomerate and how this agglomeration position is affected by fluid drag force. This reveals the radiation force profile along the length of the channel. Modelled results are used to interpret experimental results of bead deflection and trapping force.

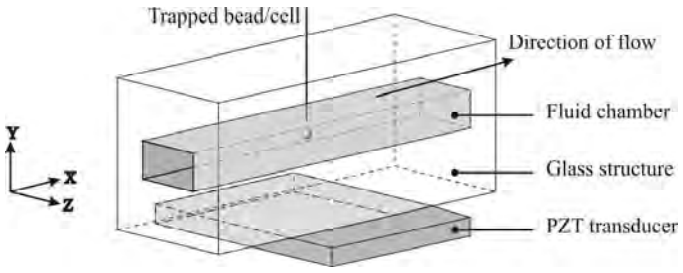

Fig. 1. Schematic of trapping device.

Results

Fig. 2 shows the predicted acoustic field pattern over half the length of the channel (symmetric about the *y*-axis). This data is used to predict the location of agglomeration sites for no-flow condition and varying levels of flow. Whilst the acoustic pressure profile is reasonably uniform around the centre of the channel, the acoustic velocity profile varies more significantly with *x* which suggests that it will generate forces which will oppose fluid drag forces. Trapping forces are also investigated experimentally using isolated resin beads. Fluid velocities of 0 to 0.42mm/s and thus Stokes' drag forces up to 500pN have been applied. Particle deflection is also measured. Both predicted and experimental data are presented in Fig. 3 showing the deflection of beads as flow rate (and Stokes' drag) is increased. In this figure the predicted Stokes' drag force has been normalized against the experimental data.

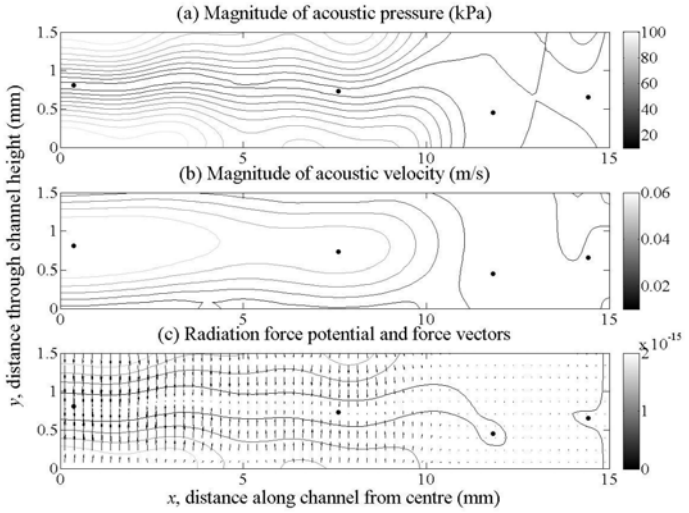

Fig. 2. Predicted patterns of (a) acoustic pressure (b) acoustic particle velocity and (c) radiation force potential and force vectors, at an excitation frequency of 455kHz no-flow conditions) plotted over half the channel length (15mm). Predicted agglomeration sites also indicated (●).

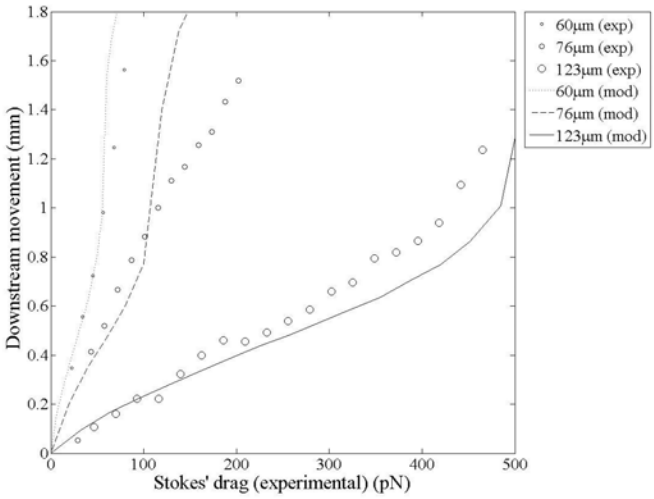

Fig. 3. Experimentally measured (exp) and modelled predictions (mod) of the spatial variation of trapping force (equal and opposite to Stokes' drag force).

Conclusions

Predictions of trapping forces acting along the length of the channel reveal the importance of the acoustic particle velocity in generating these forces. A relationship between trapping force and bead location can be established experimentally, and up to a maximum force before the bead is swept to the next trapping site or eluted. This relationship is influenced by the uniformity of the more dominant axial field and axial displacement of the bead. A similar relationship exists between the acoustic contrast (proportional to acoustic radiation force) and displacement measured. By characterizing this relationship, changes in acoustic contrast factor can be quantified, as for ion-exchange resins on exposure to counterions, by monitoring the trapping location of an isolated bead subjected to a constant flow rate.

Separation of particles by using an acoustic programming field in SPLITT channels

Mauricio Hoyos, Claire Ratier

[1]Laboratoire de Physique et Mécanique des Milieux Hétérogènes, UMR7636CNRS, ESPCI, 10 rue Vauquelin, 75005 Paris-France
hoyos@pmmh.espci.fr

Transverse ultrasonic standing wave field combined to an axial suspension flow in a Hele Shaw channel may generate a nonuniform distribution profile in the channel thickness, because of the interaction between the species and the acoustic field force. It is well known that relaxation time toward the nodes or antinodes is function of the particle size but also on the acoustic impedance contrast factor. It is not easy to conduct size-based separations of particles is thin channels only by taking advantage of the differential transverse migration during the relaxation period, by using only one ultrasonic focusing zone. In fact, too many parameters: flow rate, acoustic force, the coupling with the parabolic flow profile, have to be adjusted in order to collect fractions of different particle size at different outlets. In this presentation, we shall describe a method for size-based separation of particulate materials using ultrasonic standing wave programming. The experimental device, we shall call, Hydrodynamic-Acoustic Continuous Sorter, HACS, consists in a ribbon-like channel, we call step-SPLITT, provided with two inlets and two outlets. The sample and the carrier fluid can be injected separately and continuously at the inlets. The flow profile is laminar. Species are manipulated by a combination of gravity and ultrasonic standing wave fields acting upon particles perpendicularly to the flow. The goal is to generate transversal selective migration of species and evacuate them at different outlets. In this work we are limited to two species. The acoustic programming consists in placing two transducers of different frequencies along the channel; in this work we'll focus to this basic configuration (see Fig.1), but other configurations are possible. The channel dimensions are 5cm length, 0.5cm breadth and 400µm thick. We demonstrate that, under some flow conditions and using the effect of selectivity in relaxation time, a one node acoustic field generates a pre-separation of 5 and 10µm latex particles. A second field composed of two nodes allows achieving separation placing the smaller particles at the upper node and the bigger particles at the lower node (see Fig.1). The channel is placed horizontally and gravity acts upon particles increasing the probability separation. In this presentation we shall show the calculations predicting particle trajectories, but also a way of measuring the mean energy density in the resonator by performing experiments in microgravity. Observations *in situ* have been made using digital holographic microscopy.

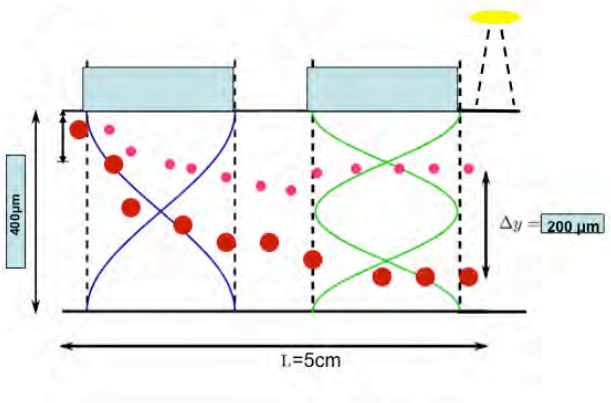

Figure 1 Schematic view of two species particle trajectories in the HACS device

Acoustic Whole Blood Plamsapheresis Chip for PSA Microarray Diagnostics

Andreas Lenshof[1], A. Ahmad-Tajudin[1], K. Järås[1,2], A-M. Swärd-Nilsson[3], L. Åberg[3], G. Marko-Varga[1], J. Malm[2,], H. Lilja[2,4] and T. Laurell[1]

[1]Lund University
Electrical Measurements
Box 118
SE-221 00 Lund
Sweden

[2] Dept. of Laboratory Medicine
Div. Clinical Chemistry
Lund University
Malmö University Hospital
Malmö, Sweden

[3]Blood Center Skåne
Lund University Hospital
Lund
Sweden

[4] Depts. of Clinical Laboratories, Surgery (Urology) and Medicine (GU-Oncology)
Memorial Sloan-Kettering Cancer Center, New York

Generating high quality plasma from whole blood is of major interest for many biomedical analyses and clinical diagnostic methods. The handling and processing of fluids with high cell content, like whole blood, in microfluidic separation devices has proven to be a major challenge often resulting in diluted samples or poor throughput. Diverse micro-technology techniques have been developed to enable separation and concentration of the different components in whole blood [1]. Extensive efforts have also been spent on the development of chips that integrate plasma generation with subsequent miniaturized diagnostic tests. In this abstract, an acoustophoresis based separation chip that prepares diagnostic plasma from whole blood and its clinical application are presented.

Previously presented microfabricated silicon acoustic separator chips has not been able to process high particle concentrations, partly due to the very high acoustic forces required to concentrate particles into a band narrow enough to enable separation in a laminar flow via flow splitting [2, 3]. A new acoustophoresis chip has been developed to deal with this limitation. Since the particles exhibits tighter focusing the longer time they remain in the acoustic field, the separation channel was elongated in a meander type of fashion, see figure. An acoustic force of higher magnitude is thus not necessary, as the radiation force instead acts for a longer duration forcing the cells gently into a focused band. The impact of the longer separation channel was investigated with four different chips with four different channel lengths.

Additionally, several extra outlets were added along the separation channel. These outlets, placed in the middle of the separation channel, allow blood cells already focused to be removed without removing a large part of the blood plasma. The cellular content in the suspension is thus lowered gradually in sequential steps, until only cell free plasma remains. Results show that the chip was able to produce plasma with sufficiently low cell content to fit the suggestions of the Council of Europe, a limit which is set to $6x10^9$ red cells/L. The total number of cells in the sample ran through the plasmapheresis chip was $3.65x10^9$, which is well below the required limit.

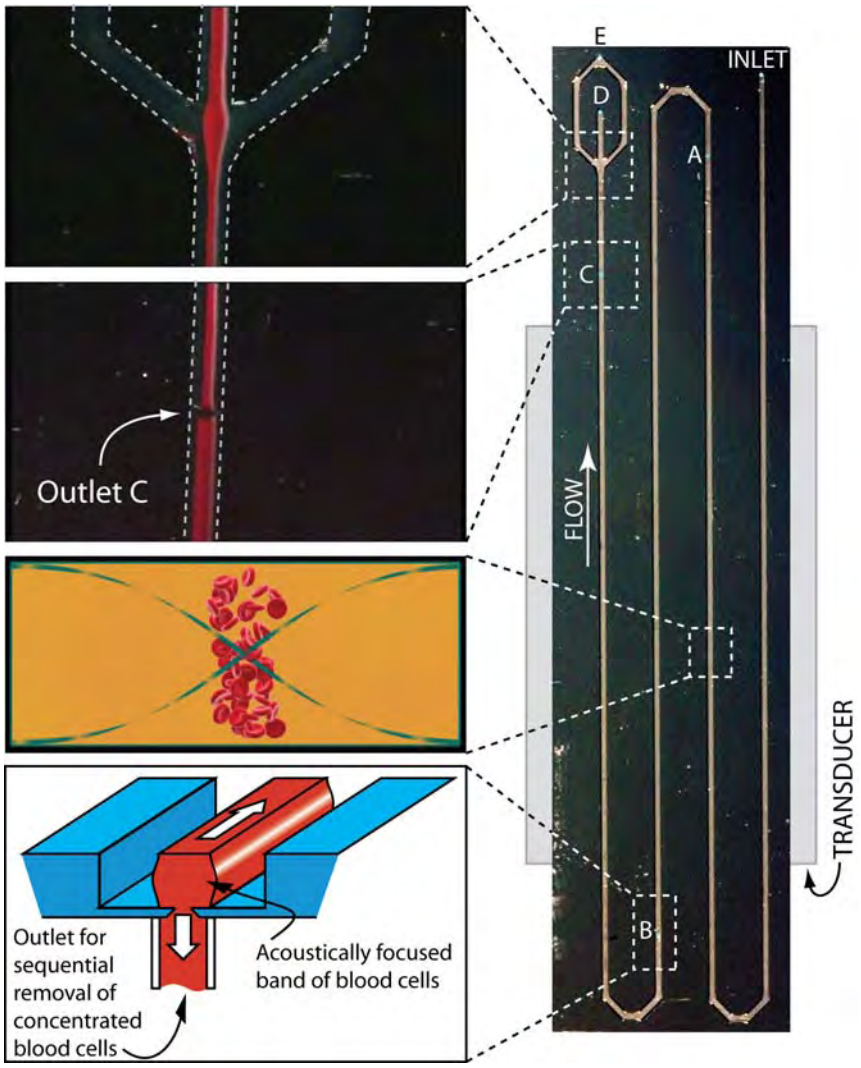

The plasmapheresis microchip was then successfully linked to a porous silicon sandwich antibody microarray chip for Prostate Specific Antigen (PSA) detection, developed in house. PSA was detectable from the generated plasma via fluorescence readout at clinically significant levels of 0.19-21.8 ng/ml with good linearity (R^2> 0.99) without any signal amplification. By combining USW microfluidics and protein microarray technology, an all microchip based PSA detection from whole blood is obtained in a novel lab-on-a-chip technique.

REFERENCES

[1] M. Toner, D. Irimia, *Annual Review of Biomedical Engineering*, **7**, 77-103 (2005).
[2] A. Nilsson, F. Petersson, H. Jonsson and T. Laurell, *Lab on a Chip*, **4**, 131-135 (2004).
[3] F. Petersson, A. Nilsson, C. Holm, H. Jonsson and T. Laurell, *The Analyst*, **129**, 938-943 (2004)

Three devices for SAW-induced particle manipulation in continuous flow systems

Linda Johansson[1], Johannes Enlund[2], Stefan Johansson[1], Ilia Katardjiev[2], Ventsislav Yantchev[2]

[1]Uppsala University
Dept. of Engineering Sciences, Microsystems
Ångström Lab
SE-752 26 Uppsala
Sweden
linda.johansson@angstrom.uu.se

[2] Uppsala University
Dept. of Engineering Sciences, Solid State Engineering
Ångström Lab
SE-752 26 Uppsala
Sweden

Surface acoustic waves (SAW) excited by interdigital transducers (IDT) on lithium niobate ($LiNbO_3$) or lithium tantalate ($LiTaO_3$) offer several advantages for acoustic particle manipulation compared with piezoceramic $PbZr_{(1-x)}Ti_xO_3$ (PZT) BAW transducer. Here, three SAW-devices are evaluated; a poly-di-metyl-sioloxane (PDMS) channel on lithium niobate, a Pyrex-channel on lithium niobate and a silicon dioxide on lithium tantalate.[1]

Introduction

SAW-excitation by IDTs is possible within a wide frequency range, at least from 15 MHz to lower GHz. According to theory, the acoustic radiation force scale linearly with the operation frequency. Hence, allowing for manipulating smaller particles, at lower voltages etc. In continuous flow operation, very small internode distances as is expected for a plane wave high frequency operation is impractical. Here, operation frequencies around 35-40 MHz is evaluated.

The position of the IDTs outside the channel, *Figure 1*, enables a thin transparent device for easy inspection and a manufacturing process compatible with planar microfabrication techniques. The large aperture of the IDT relative the wavelength enables a uniform excitation along the channel and little divergence of the acoustic field and therefore potentially a uniform acoustic field in the channel. The power density of a SAW is high, in the range of 100 W /cm^2 [2] and the coupling of a SAW from the piezoelectric substrate into the fluid by a leaky wave is an efficient coupling mechanism. The lithium niobate and lithium tantalite are associated with low material losses and therefore do not generate any considerable temperature increase in the actuator material.

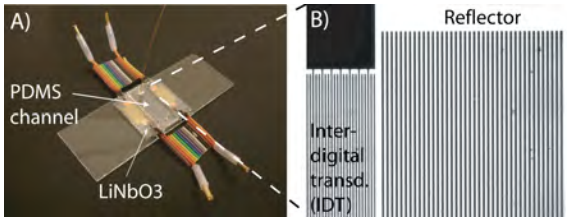

Fig. 1. *A) Typical system set-up, here for PDMS-channel and lithium niobate substrate, with the gold IDT stripes and reflector stripes (for directionality). The substrate is mounted on a microscope glass slide. Fluidic inlet was provided by a glass capillary. By connecting the electrical connections on one side the two IDTs can be operated in series. B) Close-up of the IDT strips and the reflector strips.*

The different channel materials have different advantages. PDMS enable fast prototype fabrication and ease of bonding. Pyrex glass, on the other hand, is a common microfluidic channel material, especially in industry where glass and thermoplastic polymers dominate. Compared with PDMS, glass has fundamentally different acoustic properties and the coupling of acoustic energy from a SAW into the fluid layer via the glass channel will be affected by factors such as much lower viscous losses in glass and energy build up of BAW mode resonances in the glass structure and inside the fluid due to the

high acoustic impedance of glass. The third device of silicon dioxide channel and lithium tantalite was chosen since this material combination for X-cut Z-propagation supports an interface acoustic wave (IAW) at the substrate-channel interface, *Figure 2C*. Efficient coupling of the acoustic energy into the channel is expected in this case. As can be observed in *Figure 2*, the three devices have different channel geometries.

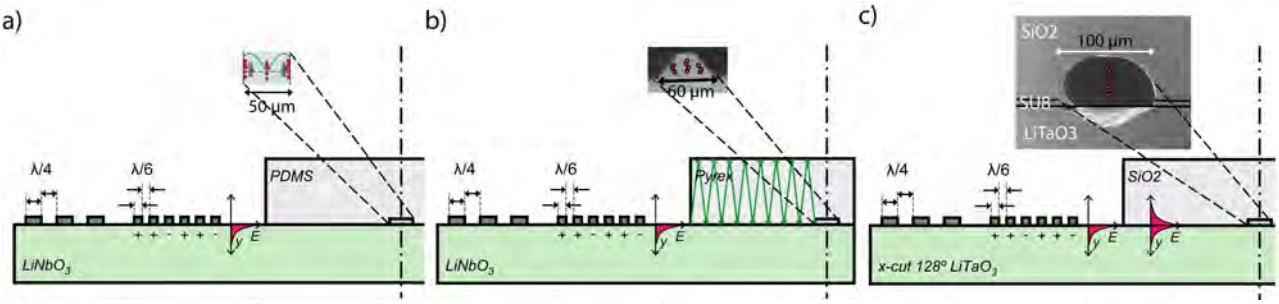

Fig. 2. *Illustration of the particle manipulation induced by surface acoustic wave (SAW) excitation into a fluid channel by interdigital transducers (IDT) and A) lithium niobate substrate and poly-di-metyl-siloxane (PDMS) channel, B) lithium niobate substrate and Pyrex glass channel and C) lithium tantalite substrate in and fused silica channel excited in x-cut y-direction that supports an interface acoustic wave (IAW).*

Results

Particle alignment

Particle alignment was observed for all three cases. 1.9 µm diameter polystyrene (PS) particles for the 1 cm long PDMS and the glass channel when operated around 9 Vpp at flow of 8-20 mm/s. The IAW-device enabled efficient alignment of 0.5 µm diameter PS particles at 13 mm/s flow when operated at 6 Vpp. No acoustic streaming was observed as observed at zero pumping flow.

Internode spacing

The pressure node spacing for the 50 µm wide PDMS channel was equal to a half wavelength of a plane wave in the fluid. This is smaller than presented elsewhere for a PDMS channel.[3] Further, this device supports particle alignment positions close to, as well as away from, the channel walls depending on device and frequency. This property is advantageous for particle manipulation to a sensor surface, when contact with the channel wall is undesired or when extracting a positive acoustic factor particle through two side outlets offer efficiency improvements.

For the 60 µm wide glass channel, the pressure node spacing was also equal to half wavelength spacing for a plane wave in the fluid. The pressure nodes where positioned symmetrically in the channel and it was possible to operate the device with only one IDT.

For the 100 µm wide IAW-device the internode distance was larger than half a wavelength for a plane wave in water, in the range of a half wavelength of a standing SAW (wavelength 100 µm). This is similar as for wall-less chambers.[4] The larger internode distance is advantageous for employing simple flow-split design for continuous flow operation at high frequency.

[1] L. Johansson, "Acoustic Manipulation of Particles and Fluids in Microfluidic Systems," in *Materials Science*. Uppsala: Uppsala University, 2009.

[2] M. K. Kurosawa, H. Itoh, and K. Asai, "Elastic friction drive of surface acoustic wave motor," *Ultrasonics*, vol. 41, pp. 271-275, 2003.

[3] J. J. Shi, D. Ahmed, X. Mao, and T. J. Huang, "Surface acoustic wave (SAW) induced patterning of micro beads in microfluidic channels," presented at Micro Electro Mechanical Systems, 2008. MEMS 2008. IEEE 21st International Conference on, 2008.

[4] C. D. Wood, J. E. Cunningham, R. O'Rorke, C. Walti, E. H. Linfield, A. G. Davies, and S. D. Evans, "Formation and manipulation of two-dimensional arrays of micron-scale particles in microfluidic systems by surface acoustic waves," *Applied Physics Letters*, vol. 94, pp. 054101, 2009.

Drop mixing and displacement by surface acoustic waves

Philippe Brunet, Michaël Baudoin, Olivier Bou Matar, Farzam Zoueshtiagh and Alain Merlen

IEMN – UMR CNRS 8520. Avenue Poincaré BP 60069 59652 Villeneuve d'Ascq Cedex, France
philippe.brunet@univ-lille1.fr

We carried out experiments of drop mixing and displacement by surface acoustic waves (SAW). The drop is in partial wetting condition, with a small contact angle hysteresis. We used a substrate with piezoelectric properties (Lithium Nyobate), in order to generate powerful SAW. The transducer is an inter-digitated transducer (IDT) which generates transverse acoustic waves propagating along the surface. The frequency is fixed by the space between each track of the IDT, and is of the order of a few tens of MHz. The properties of the material ensure that the wave is not attenuated in its direction of propagation, and that it is localized near the surface.

As such a wave hits the drop, it induces a deformation in the form of capillary waves [1,2], see Figure 2. It also induces a flow inside the drop - see Figure 3, which provides good mixing properties suitable for numerous applications. At larger amplitude, the waves can induce the drop displacement [1] and even its atomisation [1,2] into several smaller droplets.

In order to understand the intrinsic mechanisms involved in the drop displacement and inside mixing, we carried out a parametric experimental study varying the frequency and amplitude of the waves, as well as the size of the drop. We try to relate the observed motion with the surface deformation of the drop, and interpret it as a possible interplay between 'acoustic streaming' effect and radiation pressure inside the drop.

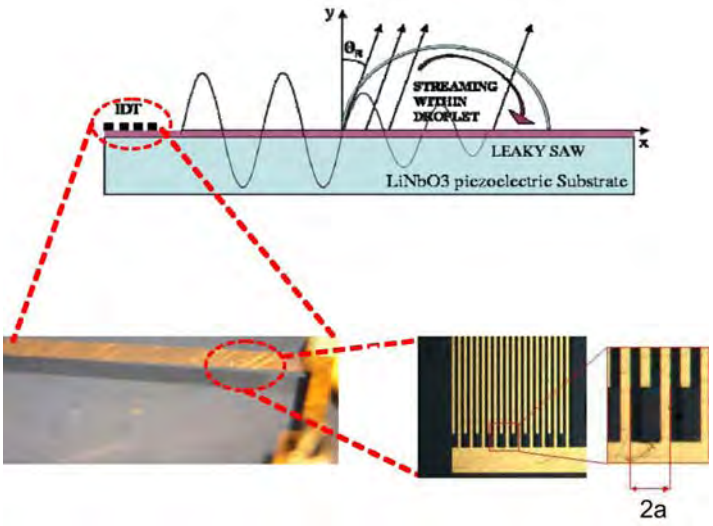

Figure 1: Scheme of the set-up. A transducer sends an ultrasonic Rayleigh wave along the substrate. The transducer (IDT) is composed of regularly spaced Titanium-Gold stripes (a=75 microns) engraved on a piezoelectric substrate. When a voltage at appropriate frequency (here about 20 MHz) is applied, the wave is produced.

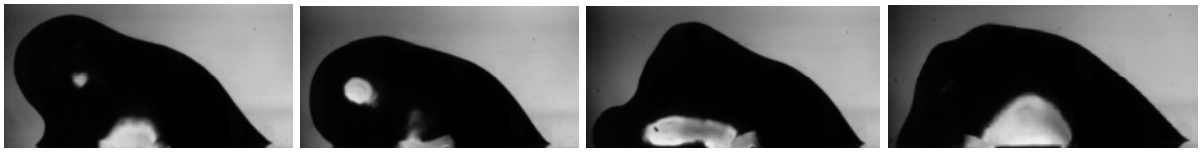

Figure 2: A sequence of drop deformation subjected to SAW. The drop moves from right to left at about 2 cm/s. f = 20.3 MHz.

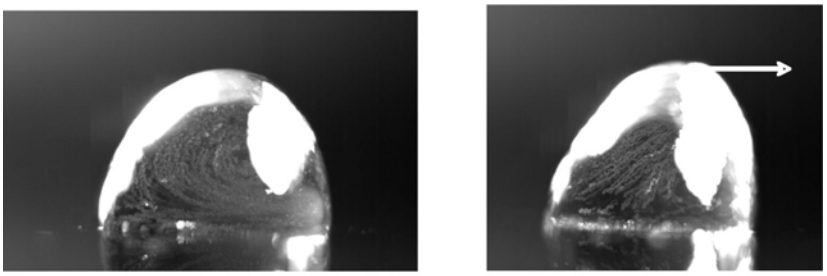

Figure 3: Detail of the flow inside the droplet

[1] A. Renaudin, E. Galopin, V. Thomy, C. Druon, F. Zoueshtiagh *Creeping, walking and jumping drop...*, Phys. Fluids **19**, 091111-1 (2007).
[2] A. Qi, L.Y. Yeo and J.R. Friend. *Interfacial destabilization and atomization driven by surface acoustic waves*. Physics of Fluids **20**, 074103 (2008).

Movement of liquids and solid particles on resonating plates

Jeremy J. Hawkes[1], Rito Mijarez-Castro[2], and Peter R. Fielden[1]

[1]School of Chemical Engineering and Analytical Science, The University of Manchester, MIB 131 Priincess Street, Manchester, M1 7DN, UK
J.hawkes@manchester.ac.uk

[2]Gerencia de Control e Instrumentación, Instituto de Investigaciones Eléctricas, CP 62490 Cuernavaca, Morelos, México.
rmijarez@iie.org.mx

Well defined vibration modes have been formed on flat plates, these modes have been visualised by placing liquids, particles or both on the surface. The vibrations move liquids to velocity antinodes and solids towards velocity nodes. The resulting pattern of heaps agree well with FE models of the vibrating plate, see figure 1. One potential application is the production of wall-less dynamic multiwall plates. Within these wells, mixing by acoustic streaming can be controlled by the applied power level.

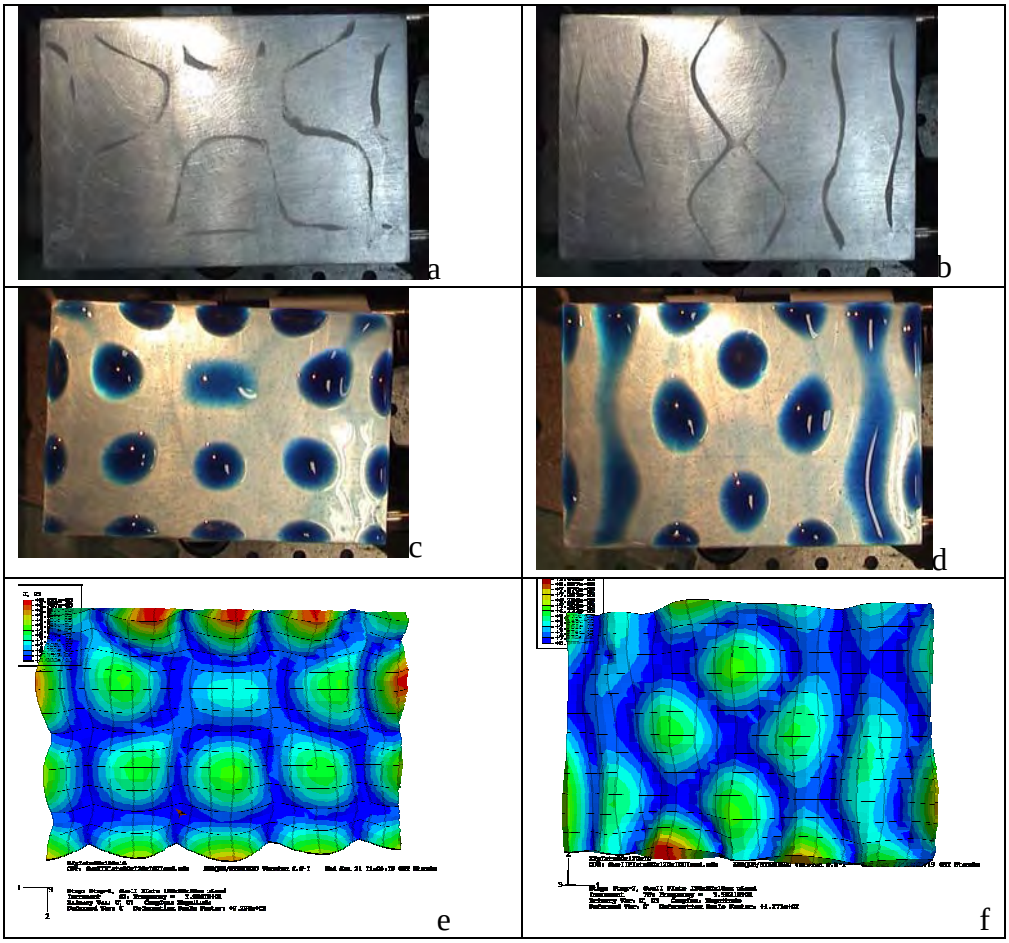

Figure 1. 120x80mm aluminium plate vibrating in two modes near 40kHz. a and b) Chladni figures formed by particles on the surface. c and d) Coloured water driven into heaps. e and f) FE (Abaqus) models of the plate vibrating near 40 kHz.

When a reflector is placed above the plate with solid particles scatted on the surface and the plate to reflector distance adjusted to create a resonance in the fluid (air) above some particles levitate and move to the same horizontal location where heaps of water would form on the surface. A protocol for creating trap patterns will be described, this uses FE modelling to select modes and then manoeuvre the modes to the desired frequency.

Map

Directions

From Stockholm International Airport (Arlanda) to KTH area:

1a) Direct train (”Arlanda Express”) to Stockholm Central Station, 240 SEK, 20 min.

or

1b) Bus (“Flygbussarna”) to ”Cityterminalen” just beside Stockholm Central Station: 110 SEK, 35 min.

and

2) Subway from Stockholm Central Station (Station ”T Centralen”) to KTH (Station ”Tekniska Högskolan”): Red line train towards “Mörby Centrum”, 40 SEK, 6 min.

Alternative: Taxi, approx. 500 SEK, 30 min (hotel address: Körsbärsvägen 1).